THE DEVELOPMENT OF FRACTURES IN THE MESOZOIC VOLCANIC ROCKS ADJACENT TO THE SIERRITA PORPHYRY COPPER DEPOSIT, PIMA COUNTY, ARIZONA

by

Randolph Charles Thompson

A Thesis Submitted to the Faculty of the

DEPARTMENT OF GEOSCIENCES

In Partial Fulfillment of the Requirements
For the Degree of

MASTER OF SCIENCE

In the Graduate College

THE UNIVERSITY OF ARIZONA

1 9 8 1

STATEMENT BY AUTHOR

This thesis has been submitted in partial fulfillment of requirements for an advanced degree at The University of Arizona and is deposited in the University Library to be made available to borrowers under rules of the Library.

Brief quotations from this thesis are allowable without special permission, provided that accurate acknowledgment of source is made. Requests for permission for extended quotation from or reproduction of this manuscript in whole or in part may be granted by the head of the major department or the Dean of the Graduate College when in his judgment the proposed use of the material is in the interests of scholarship. In all other instances, however, permission must be obtained from the author.

SIGNED: Randolph Charles Thompson

APPROVAL BY THESIS DIRECTOR

This thesis has been approved on the date shown below:

Spencer R. Titley
S. R. TITLEY
Professor of Geosciences

May 27, 1981
Date

ACKNOWLEDGMENTS

I am deeply thankful to Professor S. R. Titley for his guidance and advice in every phase of research and preparation of this thesis. I would also like to thank Professor George H. Davis and Professor John M. Guilbert for their advice and comments on the various aspects of this thesis. Funding for this project has been provided by NSF Grant EAR 78-22897.

TABLE OF CONTENTS

TABLE OF CONTENTS--*Continued*

LIST OF ILLUSTRATIONS

LIST OF ILLUSTRATIONS--Continued

LIST OF ILLUSTRATIONS--Continued

LIST OF TABLES

ABSTRACT

A description of the sequential evolution of fracture-controlled alteration assemblages in the Mesozoic volcanic rocks adjacent to the Sierrita porphyry copper system was based on detailed field observations of fractures at over 650 field station sites. Observations include fracture density, orientation, straightness and continuity, and alteration mineralogy.

Four principal fracture-controlled alteration assemblages were documented with the two younger vein sets displaying fracture densities localized about the quartz monzonite porphyry stock at the center of the Sierrita system. The two early alteration assemblages apparently reflect a distinct early hydrothermal event centered west of Sierrita. Similarities between the fracturing events suggest some general conclusions concerning the evolution of fractures in the respective systems: (1) an early, nonsulfide assemblage is related to veins attaining only moderate fracture densities and relatively widespread, irregular distribution, and; (2) a later sulfide assemblage is controlled by fractures attaining high fracture densities but relatively restricted areal extent. Finally, at least for those fractures related to the Sierrita system, the final fracture geometry appears to reflect a regional control combining with the emplacement and cooling of a generator stock.

Chapter 1

INTRODUCTION

Active geothermal systems can be of economic importance, both as energy and metal resources. This economic value is largely derived from the process of hydrothermal fluid flow. Thermal fluids are a direct energy source in active geothermal systems and are indirectly important in fossil systems, having provided a medium for complex metal ion transport. The fracturing of rocks is integrally linked to hydrothermal fluid flow (Knapp and Knight, 1977; Norton and Knight, 1977; Haynes and Titley, 1980), with fractures providing avenues for fluid movement (Norton and Knight, 1977) and potential sites for base metal localization (Anderson, 1948). Understanding fracture formation thus becomes critical to deciphering the evolution of geothermal systems.

The study of geothermal systems relies on deducing from the present condition of rocks in these systems changes produced by hydrothermal fluid flow. These rocks, and most specifically, altered and mineralized fractures and veins in them represent an end product of earlier geothermal processes (Titley, Fleming, and Neal, 1978). Progressive changes in the development of both active and fossil geothermal systems are imprinted upon altered fractures (Batzle and Simmons, 1976, 1977; Titley, 1978). By recording changes in fracture formation and hydrothermal fluid chemistry and temperature, altered fractures are measurable phenomena that provide a link in unraveling the spatial and temporal evolution of a geothermal environment (Preece, 1979; Haynes and Titley, 1980; White, 1980).

The Sierrita porphyry copper system, located about 40 kilometers southwest of Tucson, Arizona (Figure 1), has been the site of recent studies attempting to decipher the evolution of a fossil geothermal system from the study of altered fractures (Preece, 1979; Haynes and Titley, 1980; Manske, 1980; White, 1980). The Sierrita system is economically important and lacks a widespread, late-stage, texturally destructive quartz-sericite alteration envelope. The system is well-exposed, principally on a pediment surface which provides an excellent, if essentially planar cross-section of the system. Furthermore, Tertiary tilting effects appear to be relatively minor, as indicated by consistent 11 - 17^{o} south-southwest dips measures on Tertiary bedded tuffs by the author south of the deposit.

Initial studies developed the basic methodology for describing altered fractures in terms of space, time, and temperature, and were applied to portions of the district with relative structural simplicity and lithologic homogeneity (Preece, 1979; Haynes and Titley, 1980). Succeeding efforts at the Sierrita-Esperanza deposit have subsequently encountered greater structural and lithologic complexities that affected the evolution of the geothermal system (Manske, 1980; White, 1980).

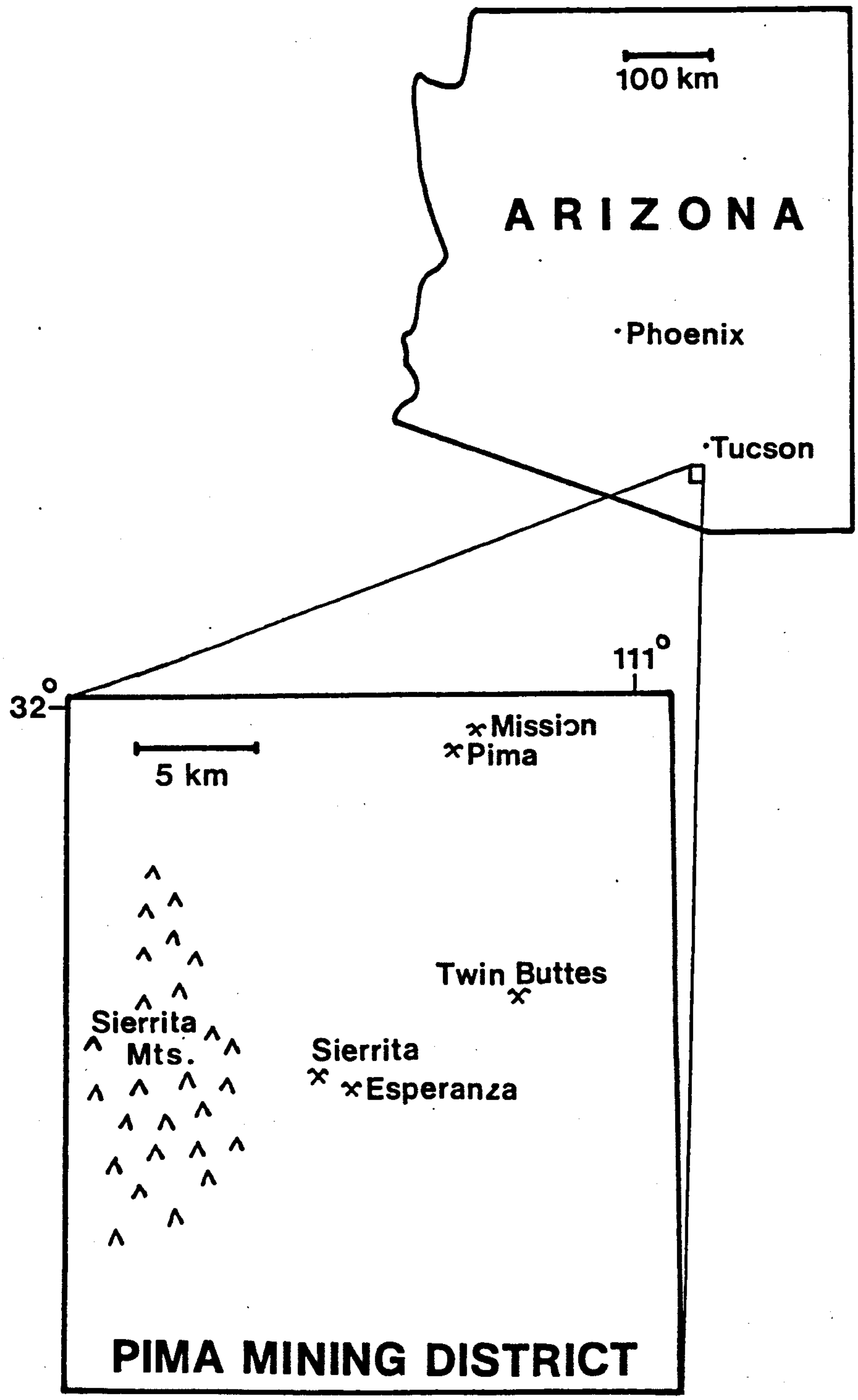

Figure 1. Location Map of the Sierrita Porphyry Copper Deposit.

The present effort continues the fracture study to the Mesozoic Ox Frame and Demetrie Volcanics and the Red Boy Rhyolite encircling the southern half of the Sierrita porphyry copper deposit and the adjacent, genetically-related Esperanza orebody (Figure 2). Using the framework provided by previous workers, fractures in the Mesozoic volcanic rocks are described in space and time, and the effects of faulting and lithologic heterogeneity examined. The results are then compared with data collected in the Tertiary Ruby Star Granodiorite north of the deposit (Haynes and Titley, 1980; Manske, 1980) and the Jurassic Harris Ranch Quartz Monzonite to the west (Preece, 1979; White, 1980). A sequential evolution of fractures is developed for the Mesozoic volcanic rocks south and west of the Sierrita system, and general explanations advanced concerning fracture formation.

The Sierrita porphyry copper system presents a known mineralizing center to which the study of fractures in the near vicinity can be related. From an exploration standpoint, the reverse of this process is of critical importance--relating a study of altered fractures to an unknown mineralizing center. The Sierrita Mountains apparently provide just such a case-study. A major goal of the present effort has been to attempt to locate a possible source for a distinct early event (White, 1980) that produced hydrothermally altered fractures spatially distributed west of the Sierrita system.

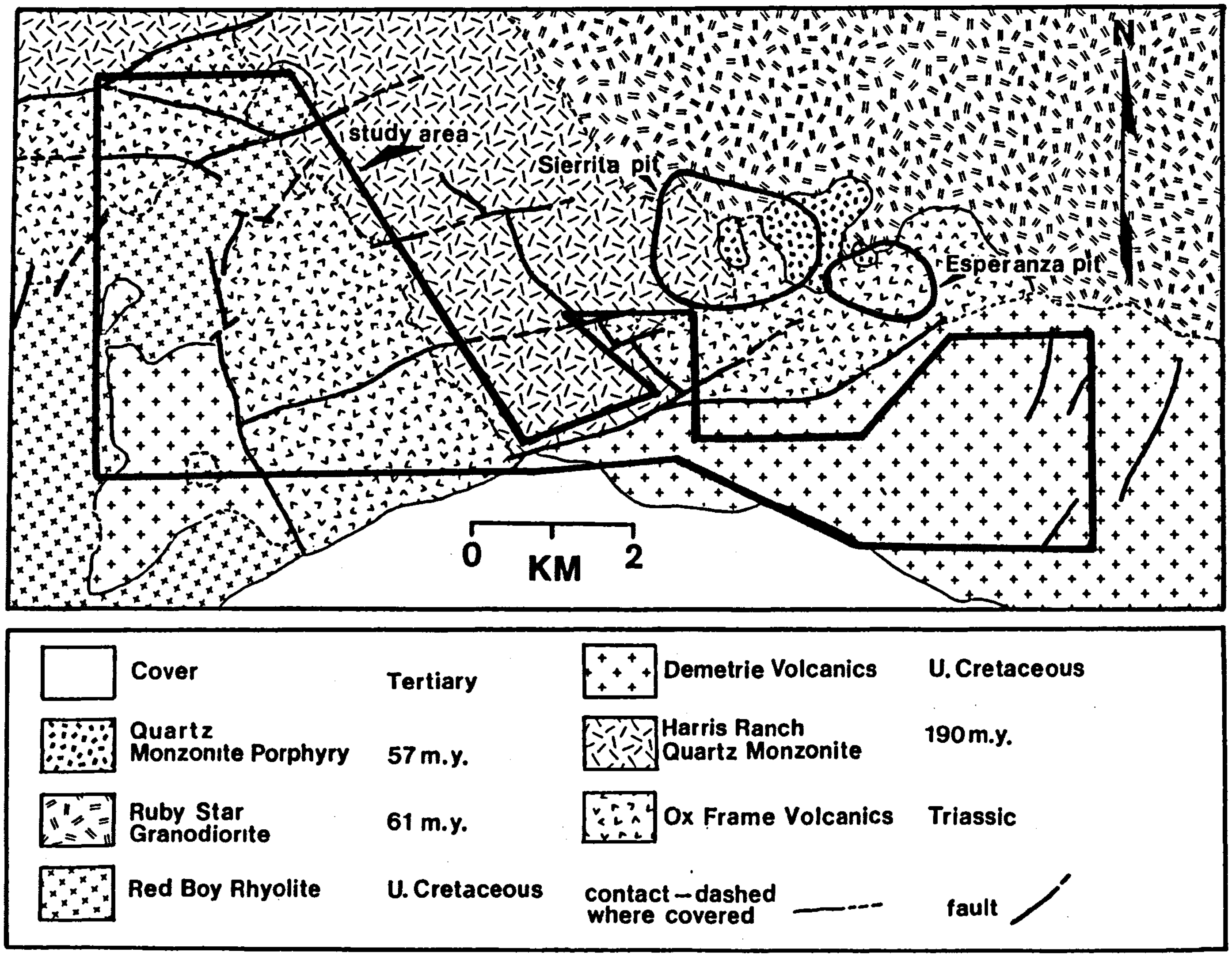

Figure 2. General Geology of Study Area.

Chapter 2

METHODS OF STUDY

Fracture data collection involved measurements at over 650 field station sites chosen on the basis of spacing relative to neighboring stations, distance from the intrusive center, and outcrop availability (Figure 3). Six parameters were measured at each site, as constituted by a 0.25 square meter circle traced on the outcrop: fracture-controlled alteration mineralogy, fracture density and orientation, crack straightness and continuity, and vein paragenesis where determinable.

Measurement techniques employed in the present study generally correspond to those utilized by other workers in the area (Haynes and Titley, 1980; White, 1980). Fracture straightness and continuity were not examined previously, necessitating a new classification scheme for these variables. Fracture density is given in units of inverse centimeters, and was derived by dividing the length of fractures within the reference circle by the area of the circle (Snow, 1970; Titley, Fleming, and Neal, 1978). A density is then computed for each fracture-controlled alteration assemblage. The integrated fracture density for that station then becomes the sum of fracture densities for each alteration assemblage

(Haynes and Titley, 1980). Straightness and continuity variables were computed for the entire length of measured fractures both in and out of the reference circle, and divided into four general categories and assigned numbers from 1 to 4. The end members of this division approximate fracture-style divisions employed by Heidrick and Titley (in press), whereby fracture styles are grouped into three basic categories: (1) J1, planar, continuous fractures corresponding to straightness and continuity values of 3 or 4 in the present usage; (2) J2, irregular, discontinuous fractures, here corresponding to straightness and continuity values of 1, and; (3) J3, microfractures, which were not recorded in the present study. Specifically, the basic categories of individual fracture continuity are as follows: (1) values of 1 were assigned to fractures that were traceable for one-half meter or less; (2) continuity values of 2 were given to fractures traceable for about 1.5 meters; (3) fractures continuous for lengths of up to 3.0 meters correspond to values of 3, and; (4) fractures traceable for more than 4.0 meters were assigned continuity values of 4. Individual fracture straightness was resolved into four basic categories by bounding extremes in fracture orientation within parallel lines approximating the average strike direction of the fracture. The width of this imaginary envelope, divided by the length of the fracture, thus becomes a measure of fracture straightness. This measurement can be correlated with an angular deviation by approximating an idealized S-shaped curve to the fracture and computing the angle between the inflection tangent and the average strike direction. Figure 4 illustrates these two methods for deriving a value for crack straightness, and demonstrates the four general categories employed in the field for individual fractures: (1) a straightness value of 1 was assigned to fractures with an approximate envelope width over length deviation measurement of about 0.15; (2) a straightness value of 2 was assigned to fractures with a deviation measurement of about 0.10; (3) fractures with deviations of about 0.05 correspond to a straightness value of 3, and; (4) fractures with a deviation measurement of ≤ 0.01 were assigned a value of 4. These categories correspond to angular deviations of approximately 30°, 20°, 10°, and 1°, respectively.

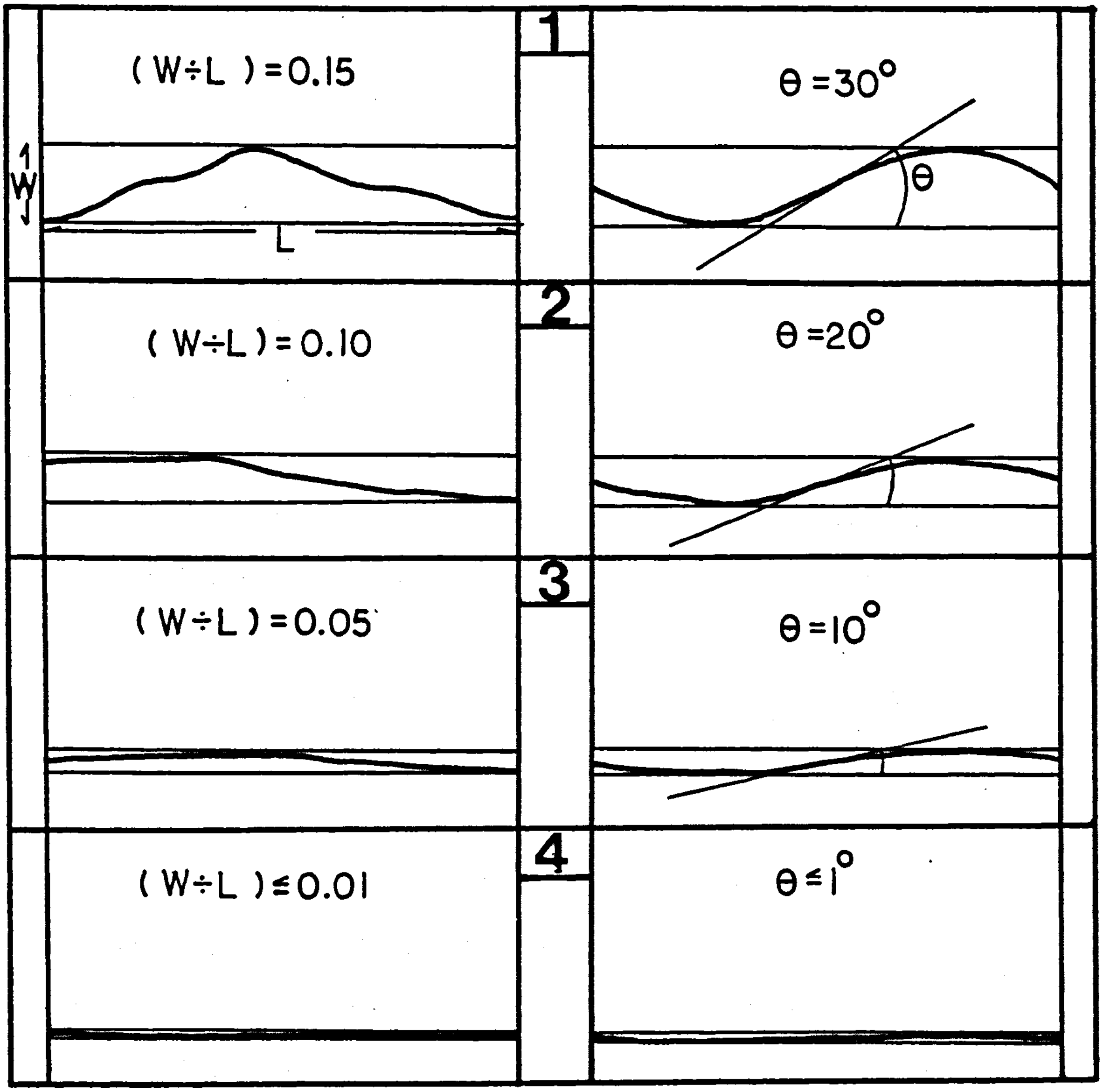

Figure 4. Classification of Fracture Straightness. -- Left column illustrates the envelope width divided by fracture length method. The right column illustrates corresponding angular deviation measurements for the four basic categories.

Chapter 3

GENERAL GEOLOGY

The Sierrita porphyry copper system lies on the east flank of the Sierrita Mountains at the southern end of the Pima Mining District (Figure 1). Various aspects of the general geology and mineralization at the Sierrita porphyry system have been described in the literature (Lacy, 1959; Cooper, 1960; Lynch, 1966, 1968; Cooper, 1971, 1973; Aiken and West, 1978; Haynes and Titley, 1980; White, 1980) and are only briefly summarized here.

Laramide-age mineralization occurs within a Mesozoic/ Tertiary complex of intrusive and extrusive rocks. Pre-Laramide-age rocks hosting mineralization are the Triassic Ox Frame Volcanics, located south and west of the Sierrita porphyry system, and the Jurassic Harris Ranch Quartz Monzonite, a 190 million year old intrusive body exposed on the west side of the Sierrita system (Cooper, 1973). The Ox Frame Volcanic unit consists principally of andesitic to rhyolitic flows and rhyolitic tuffs and is an important host to mineralization in the Esperanza orebody southeast of the Sierrita open pit. The Harris Ranch Quartz Monzonite is a medium-grained, equigranular intrusive rock and hosts mineralization in the Sierrita orebody. Other pre-Laramide-age rocks in the vicinity of the Sierrita porphyry system include the Demetrie Volcanics, formerly called the Silver Bell Formation (Lootens, 1966), and the Red Boy Rhyolite. The Demetrie Volcanics of upper Cretaceous (?) age, composed primarily of andesitic flows, are exposed south and west of the Sierrita porphyry system, generally peripheral to the Ox Frame Volcanics. Red Boy Rhyolite pyroclastics and flows, the youngest Cretaceous formation in the area, form the bulk of the crest of the Sierrita range.

Laramide-age intrusive activity in the Pima district occurred between 67 and 53 (?) million years ago (Damon and Mauger, 1966; Cooper, 1973), commencing with the intrusion of several quartz diorite stocks, followed by emplacement of the 58 (?) million year old Ruby Star Granodiorite, a batholithic body extending some 40 kilometers northwestward from the Sierrita system, and culminating with the intrusion of a biotite quartz monzonite porphyry, a possible differentiate of the Ruby Star Granodiorite. This quartz monzonite porphyry body, forming a 2-kilometer diameter stock at the southern edge of the batholith, is spatially associated with copper mineralization, and has been interpreted as the generator stock for the Sierrita porphyry copper system (Haynes and Titley, 1980).

Recent studies indicate that whole-scale fracturing of rocks is not confined to the known ore zone, but extends more than five kilometers from the center of the Sierrita porphyry system and demonstrates a temporal, spatial, and temperature association with the quartz monzonite porphyry and its intrusion 53 (?) million years ago (Damon and Mauger, 1966; Haynes and Titley, 1980; Manske, 1980, White, 1980). The present study reveals that widespread rock fracturing has occurred south of the generator stock in the Ox Frame and Demetrie Volcanics, and, despite lithologic heterogeneity and anisotropy complicated by faulting, demonstrates a spatial association with the generator stock consistent with fracture patterns noted to the north in the intrusive igneous host rocks.

Volcanic Rock Types

Mesozoic volcanic rocks exposed south and west of the Sierrita porphyry system were examined in an attempt to document the development of fractures preserved in the differing rock types. The various lithologies have been described by Cooper (1971) and are summarized here.

The Ox Frame Volcanics, as exposed in the study area, comprises metamorphosed and altered rhyolitic to andesitic volcanic rocks with relatively minor lenses of quartzite. Cooper distinguishes three members of this formation with a total minimum thickness of about 1200 meters: (1) a lower third characterized by light-grey to pale-red rhyolitic flows; (2) a middle member of medium dark-grey to dark greenish-grey andesite and dacite flows and a few flow breccias, and; (3) an upper third consisting of light-grey to medium dark-grey rhyolitic tuffs and flows that contain interbeds of quartzite.

Exposures of this formation available for study lie principally to the west of the Harris Ranch Quartz Monzonite, more than four kilometers west of the Sierrita generator stock. The bulk of the Ox Frame Volcanics formerly exposed in the immediate mine vicinity are now covered by dump material, with the exception of some hills about two kilometers southwest of the quartz monzonite porphyry stock. Rocks in these hills appear to belong at the boundary between the upper and middle members, consisting of approximately equal areas of altered rhyolitic and dacitic flows with minor tuffs, quartzites, and andesitic flows. Banding in the volcanics exposed in the hills near the Sierrita orebody is absent or poorly developed, and bedding in the quartzites is obscure. All the rock types exposed in this area form resistant outcrops, with the boldest relief provided by quartzite-capped hills.

The Demetrie Volcanic unit, a thick sequence of andesitic to dacitic flows and breccias locally containing conglomerate and rhyolitic tuff, lies in angular unconformity to the Ox Frame Volcanics. The conglomerate forms only a very minor part of the Demetrie Volcanics exposed in the study area, the vast majority being comprised of andesite flows and homogeneous breccias. A distinctive andesitic breccia is exposed near Red Boy Peak. This moderately indurated rock appears to contain at least two types of andesite clasts and rare rhyolite clasts of unknown origin, and is at least partly intrusive. Cooper (1971) describes a two-andesite breccia that he interprets to be of mudflow origin. Two conspicuous rhyolitic members occur in the Demetrie Volcanics. The lower member is a firmly-welded tuff about 230 meters thick capping prominent hills southeast of the Esperanza open pit. The lower rhyolitic member consists of poorly-welded tuffs and probable ash fall material. With the exception of the lower rhyolitic member, the Demetrie Volcancis forms a recessive topography and is generally poorly exposed. Cooper (1971) estimates a possible 2400 meter thickness for the Demetrie Volcancis south of the Sierrita system, thinning and pinching out underneath the Red Boy Rhyolite northwestward, toward the core of the range.

The Red Boy Rhyolite unconformably overlies the Demetrie Volcanics and is in turn unconformably overlain by gravel and basaltic andesite of middle Tertiary age. This extremely resistant formation comprises the core of the Sierrita Mountains, capping several high peaks. The Red Boy Rhyolite is composed of rhyolitic tuff and tuff breccia containing intercalated rhyolitic flows. Lobo Peak, located about a mile south of Red Boy Peak, marks a general latitude corresponding to a change in the Red Boy Rhyolite from a pinkish-grey to pale-red argillized facies south of the Sierrita Mountains to a hard, light-grey metamorphosed facies in the core of the range. Metamorphic effects documented by Cooper (1971), identifiable only in thin section, include strained phenocrysts, microfaulting, and microveining oblique to earlier compaction foliation.

Structure

The principal structural elements of the area are faults and intrusive contacts. Faulting is generally hi-angle, with a major exception being a NW-trending structure located west of the Sierrita open pit with observed dips of 39° - 75°. This pre-mineralization fault is characterized by intense shearing as marked by a chloritically-altered foliated zone of up to 20 meters wide along its length. This structure is offset with a left-separation motion by ENE-trending, near vertical faults. These mineralized structures exhibit both normal and low-angle west-dipping slickenslides. Mineralized faults south and east of the Sierrita porphyry copper deposit dip steeply to the northwest. Other NE-trending faults have been interpreted by Weaver (1971), who, on the basis of seismic profiles and drill core information, proposed the existence of three or four graben-type structures "arrayed" along the fringe of the batholith from the Ruby Star ranch northward. The ENE and NE trends of faults near the Sierrita system are also the dominant fracture strike directions in the Sierrita and Esperanza open pits, respectively (Smith, 1975, Aiken and West, 1978). Some major WNW-trending faults are also present, principally in the Sierrita Mountains west of the open pits. Lootens (1966) speculates that the emplacement of the 53 (?) million year old quartz monzonite stock associated with copper mineralization was localized by the intersection of ENE- and WNW-trending structures. Intrusive contacts are obscure, but the consistency of the NW-trending strike directions of the Harris Ranch Quartz Monzonite and the Ruby Star Granodiorite suggests a hi-angle orientation.

The Red Boy Rhyolite occurs in a structurally complicated depositional setting. This unit lies in a linear, NNE-trending complex graben bounding the core of the Sierrita Mountains that probably formed, at least in part, during deposition of the rhyolite (Cooper, 1971). Cooper has interpreted Lobo Peak to be a volcanic vent based on the necklike form of the rhyolitic core and on the presence of lithologically identical Red Boy Rhyolite tuff found in small intrusive bodies in the Demetrie Volcanics nearby. The Demetrie Volcanics found in the complex graben contain patches of intense quartz-sericite hydrothermal alteration, especially in the vicinity of Red Boy Peak. These zones generally have circular to elliptical shapes and are usually on the order of several meters in diameter. Original rock textures have been destroyed in these zones of hydrothermal alteration. They contain sporadically distributed breccias characterized by white, angular, silicified clasts, 0.5 - 3.0 centimeters in diameter set in a white to reddish-purple silicified matrix. Two persistent linear belts of hydrothermal alteration occur, one trending NNE and the other NNW, roughly cradling the western flank of Red Boy Peak. Although the hydrothermal alteration zones do not appear to extend into the Red Boy Rhyolite, the rhyolitic rocks are more intensely fractured along the southwest flank of Red Boy Peak, the general vicinity of the most abundant and extensive alteration.

Chapter 4

FRACTURE-CONTROLLED ALTERATION ASSEMBLAGES

Five distinct fracture-controlled alteration assemblages are present in the Mesozoic volcanic rocks surrounding the Sierrita porphyry system. From earliest to latest, with minerals listed in order of decreasing abundance, the following paragenetic sequence was observed: (1) early epidote±quartz±chlorite±trace sulfide vein filling, usually with a selective K-feldspar±chlorite halo; (2) early sulfide±quartz±K-feldspar±epidote±chlorite vein filling, occasionally with a selective K-feldspar±quartz halo; (3) quartz±epidote±K-feldspar±chlorite±trace suflide vein filling, rarely with a selective ±K-feldspar±quartz halo; (4) quartz±sulfide±epidote±K-feldspar vein filling, rarely with a selective feldspar±quartz halo, and; (5) late calcite vein filling. Mineralogy tends to vary between differing rock types (Table 1), but various assemblages can be grouped into specific paragenetic alteration sets on the basis of overall similarities in composition and consistent crosscutting relationships. The presence of a K-feldspar halo, chlorite as a common accessory mineral, and epidote even in the silicic volcanic rocks helps distinguish the early epidote+quartz +K-feldspar and sulfide+quartz+K-feldspar alteration assemblages

Table 1. Fracture-controlled Alteration Assemblage Mineralogy. -- Abbreviations: MVSW=Mesozoic volcanic rocks south and west of the open pits (present study); RSNW=Ruby Star Granodiorite northwest of the Sierrita open pit (Haynes and Titley, 1980); RSNE=Ruby Star Granodiorite northeast of the Esperanza open pit (Manske, 1980); HRIP=Harris Ranch Quartz Monzonite in the open pit (Preece, 1979); HRWP=Harris Ranch Quartz Monzonite west of the Sierrita open pit; TRos=Ox Frame Volcanics quartzite; TRo=Ox Frame Volcanics rhyolite; TRoa=Ox Frame Volcanics andesite; Kdr=Demetrie Volcanics rhyolite; Kd=Demetrie Volcanics andesite; Kr=Red Boy Rhyolite; Trs=Ruby Star Granodiorite; Jhr=Harris Ranch Quartz Monzonite; Bio=biotite; Cal=calcite; Chl=chlorite; Cpr=chalcopyrite; Ep=epidote; Hem=hematite; Ksp=K-feldspar; Py=pyrite; Qtz=quartz; Ser=sericite; Sulf=sulfide.

Table 1. Fracture-controlled Alteration Assemblage Mineralogy

		EARLY →								→ LATE
		MINERALOGY: VEIN FILL/HALO								
Data Source	Rock Type	Set 1	Set 2	Set 3	Set 4	Set 5	Set 6	Set 7	Set 8	Set 9
MVSW	TRos	Qtz±Ep±Ksp ±Chl ±Ksp±Chl halo	Sulf±Qtz±Ksp ±Ep±Chl ±Ksp±Qtz halo	Qtz±Ksp	Qtz+Sulf±Ksp					Cal
	TRo	Ditto	Ditto	Qtz±Ksp±Ep ±Qtz halo	Qtz+Sulf±Ksp ±Ep					Cal
	TRoa	Ep±Qtz±Ksp ±Chl	Sulf±Qtz±Ksp ±Ep±Chl	Qtz±Ep±Ksp ±Ksp±Qtz halo	Qtz+Sulf±Ep ±Ksp					Cal
	Kdr			Qtz±Ksp±Chl	Qtz+Sulf±Ksp ±Chl					Cal
	Kd	Ep±Qtz±Ksp ±Chl	Sulf±Qtz±Ksp ±Ep±Chl	Ep±Chl±Ksp ±Qtz ±Ksp halo	Ep+Sulf±Qtz ±Ksp±Chl ±Ksp halo					Cal
	Kr	Qtz±Ksp±Ep ±Ksp halo	Sulf±Qtz±Ksp							Cal
RSNW	Trs			Ksp+Qtz	Qtz+Py	Py+Qtz	Ksp+Ep			
RSNE	Trs			Ksp+Qtz+Mgt	Qtz+Py	Py+Cpr +Ser	Qtz+Ksp +Ep+Chl		Qtz+Ep +Chl	
HRIP	Jhr			Qtz+Ksp+Bio +Hem	Qtz+Ep +Chl+Sulf	Qtz+Ep +Chl+Sulf	Qtz+Ep +Chl+Sulf	Qtz+Ser +Sulf		
HRWP	Jhr	Ep+Qtz ±Ksp±Chl halo			Qtz+Ksp +Py	Py+Qtz	Ep±Ksp			

from the mineralogically similar quartz+epidote+K-feldspar and quartz+sulfide assemblages, respectively. Separation of the two early alteration assemblages is further aided by a spatial distribution in marked contrast to that of the younger sets. The four assemblages can be found together only in a very small area about four kilometers southwest of the generator stock of the Sierrita system. This area marks the western limit of the quartz+epidote+K-feldspar and quartz+sulfide alteration assemblages and the southeastern limit of the early epidote+quartz+K-feldspar and sulfide+quartz+K-feldspar sets.

Changes in mineralogy of the fracture-controlled alteration assemblages in the various rock types are usually consistent for all of the sets. Epidote and chlorite become more predominant constituents with increasingly basic rock compositions and is often completely absent in the silicic rocks. The most radical difference in mineralogy occurs in the andesites of the Demetrie Volcanics, in which quartz is a volumetrically minor component of the two younger assemblages, contrasting with all other rock types.

Chapter 5

DISCRIMINATION OF AN EARLY HYDROTHERMAL EVENT

In his study of the Harris Ranch Quartz Monzonite west of the Sierrita open pit, White (1980) identified a probable early hydrothermal event that produced a fracture-controlled alteration assemblage of epidote+quartz+chlorite vein filling with a selective ±epidote±K-feldspar±chlorite halo. This conclusion was based on several lines of evidence characterizing the early assemblage: (1) fracture distribution patterns inconsistent with later assemblages; (2) generally westward-increasing fracture densities up to six kilometers from the Sierrita generator stock; (3) higher fluid inclusion temperatures in this assemblage at 5.8 kilometers than at 3.5 kilometers from the Sierrita center; (4) sharp differences in fracture orientations between this assemblage and later ones, and; (5) the lack of a corresponding assemblage in the Ruby Star Granodiorite.

On the basis of the preceding observations, White (1980) proposed the existence of an early hydrothermal event. The earliest fracture-controlled alteration assemblage noted in the Mesozoic volcanic rocks of the present study is almost identical in composition to White's early set. The easternmost occurrence of this set in the volcanic rocks is about 3.0 kilometers west of the Sierrita generator stock. The second, sulfide alteration assemblage resembles the earliest assemblage with the exception of sulfide as a major constituent. The early sulfide set is first seen about 3.5 kilometers west of the Sierrita mineralizing center, with an increase in fracture density to the west. The observed paragenetic relationships, distinctive alteration assemblage mineralogies, fracture distribution and orientations, and fluid inclusion data combine to suggest an early hydrothermal event centered west of the Sierrita generator stock. A major goal of this study was to attempt to locate a possible source area for this early event by applying the principles derived in conjunction with the study of fracturing related to the Sierrita mineralizing center.

Chapter 6

FRACTURE-CONTROLLED ALTERATION ASSEMBLAGES SPATIALLY RELATED TO THE SIERRITA GENERATOR STOCK

The quartz+epidote+K-feldspar and quartz+sulfide fracture-controlled alteration assemblages demonstrate a spatial association with the quartz monzonite porphyry stock at Sierrita, with high fracture densities localized about this center. Correlated assemblages in the intrusive host rocks (Table 1) display decreasing fluid inclusion temperatures with distance from the intrusive center (Manske, 1980; White, 1980). The previous studies have noted two alteration assemblages containing sulfide. Generally poor preservation of alteration assemblages precludes consistent documentation of two distinct sulfide assemblages in the Mesozoic volcanic rocks that might be distinguished by the relative abundance of sulfide. Consequently, two probable sets have been analyzed as a single sulfide alteration assemblage.

Fracture Orientations

Fracture orientations are represented by strike histograms, contoured Schmidt equal-area lower hemisphere stereographic projections, and by plan-view maps of averaged dominant strike directions measured at individual station sites.

Fracture strike directions are generally dominated by ENE orientations, with domain-related complications to this pattern present within and between the two alteration assemblages. A combined plot reveals a strong ENE orientation maximum (N70E $\pm$ 10°), with a pronounced NE maximum (N35E $\pm$ 10°), and weaker N80W $\pm$ 10° and N10W $\pm$ 5° peaks (Figure 5). The ENE trend, present in many other porphyry copper deposits of southern Arizona (Rehrig and Heidrick, 1972; Heidrick and Titley, in press), is especially well expressed in the sulfide assemblage (Figure 6). Differences in fracture orientations for the assemblages are especially apparent when examined by domains. The ENE strike direction is totally dominant for the sulfide assemblage to the west, whereas N40E $\pm$ 10° and N10W $\pm$ 5° trends are also present to the south (Figure 7). The nonsulfide assemblage has well developed ENE and NE orientation maxima in the western domain and a N20W $\pm$ 10° strike direction peak, in contrast with less pronounced ENE and WNW peaks to the south (Figure 8).

These domain-related fracture orientation differences require that the effect of rock type on strike directions be examined for the Ox Frame Volcanics in the western domain. There, andesite flows, dacite to rhyolite flows and tuffs, and quartzites are interlayered and well-exposed in a small area. Fracture orientations are remarkably similar among the various rock types (Figure 9), especially considering the relatively small data base available.

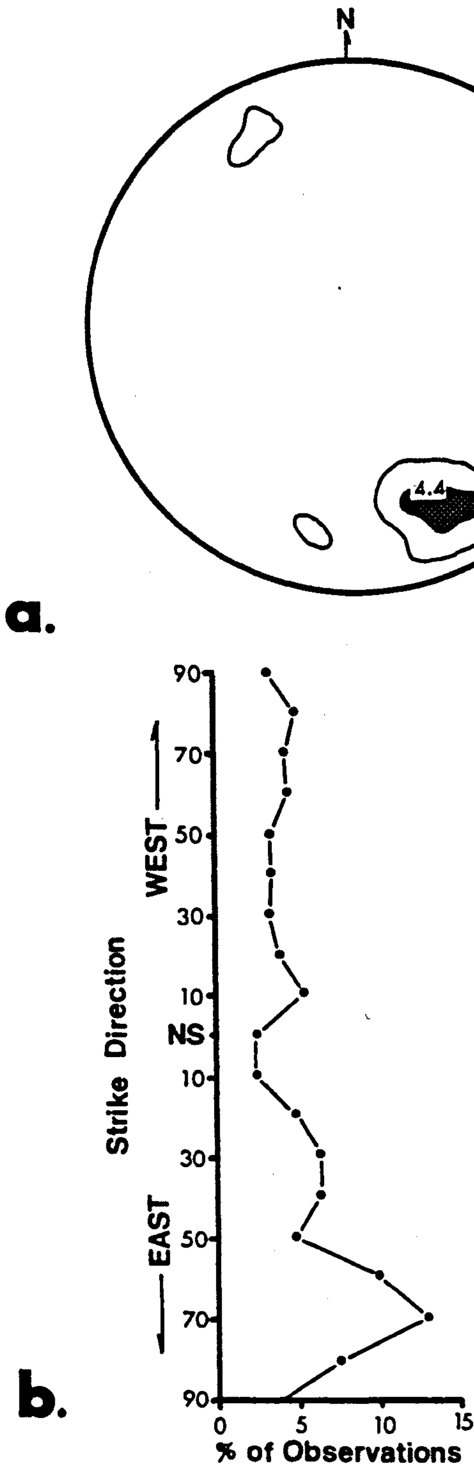

Figure 5. Orientations of Sierrita-related Fractures. -- Based on 1331 data points. Contoured per 1% of area. Contour interval=2.2%.

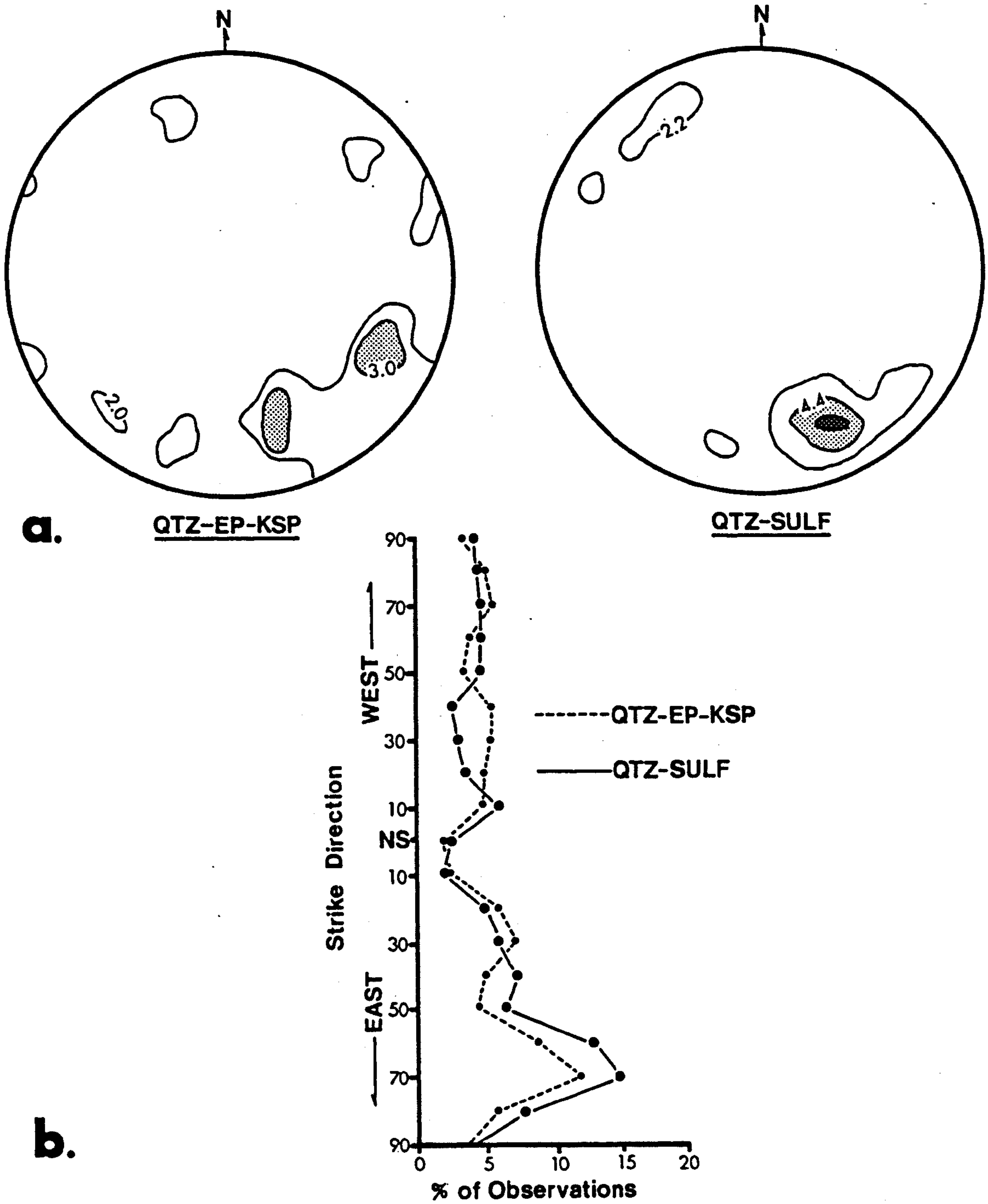

Figure 6. Fracture Orientations of the Quartz+Epidote+K-feldspar and Quartz+Sulfide Alteration Assemblages. -- (a) pi diagrams; (b) strike histogram Qtz-Ep-Ksp=416 points Qtz-Sulf=915 points Contoured per 1% of area. Contour interval=2.0% and 2.2% for the Qtz-Ep-Ksp and Qtz-Sulf assemblages, respectively.

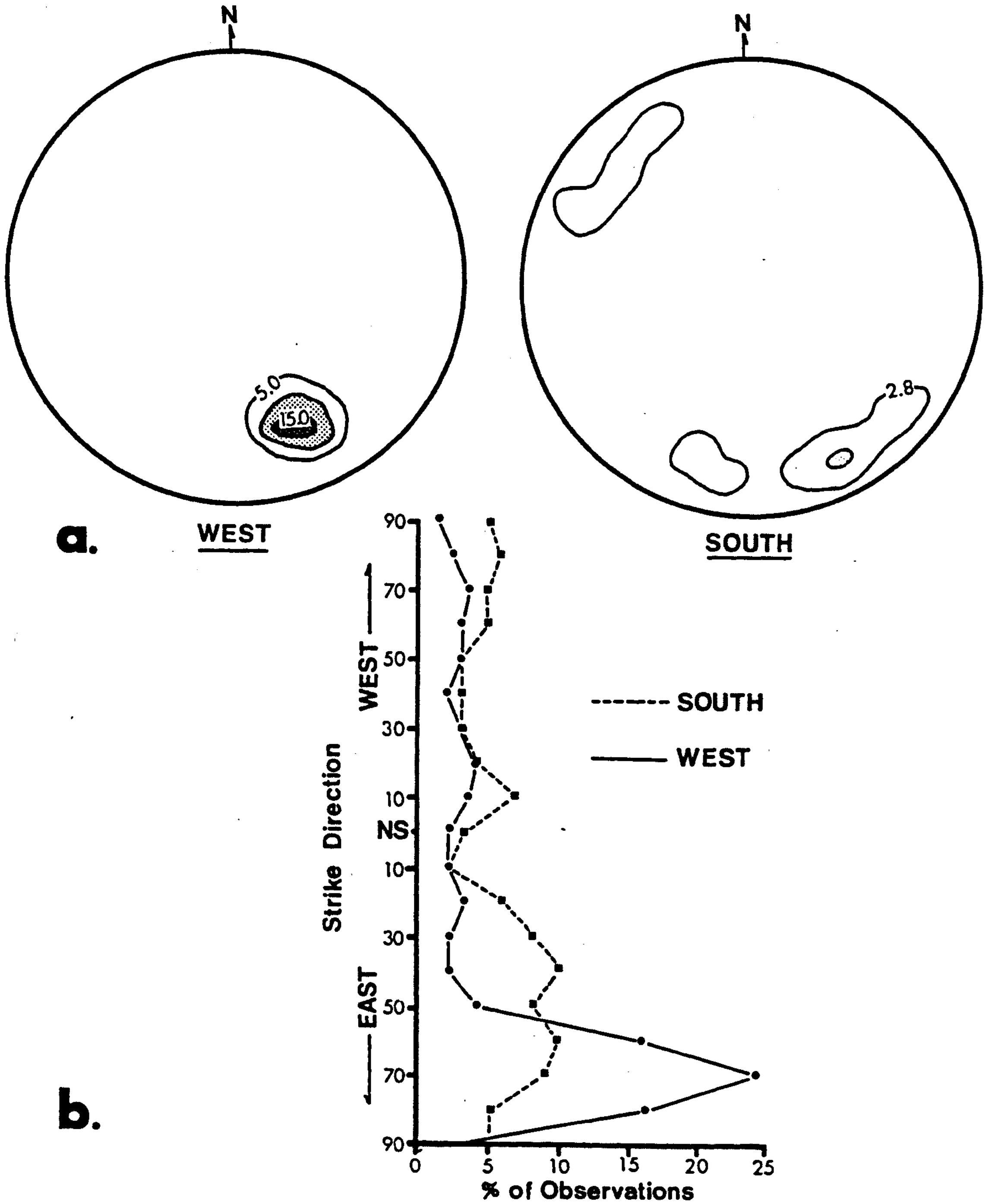

Figure 7. Domain-related Fracture Orientations of the Quartz+Sulfide Alteration Assemblage. --
(a) pi diagrams (b) strike histogram
West=282 points South=633 points
Contoured per 1% of area. Contour interval=5.0% and 2.8% for the West and South domains, respectively.

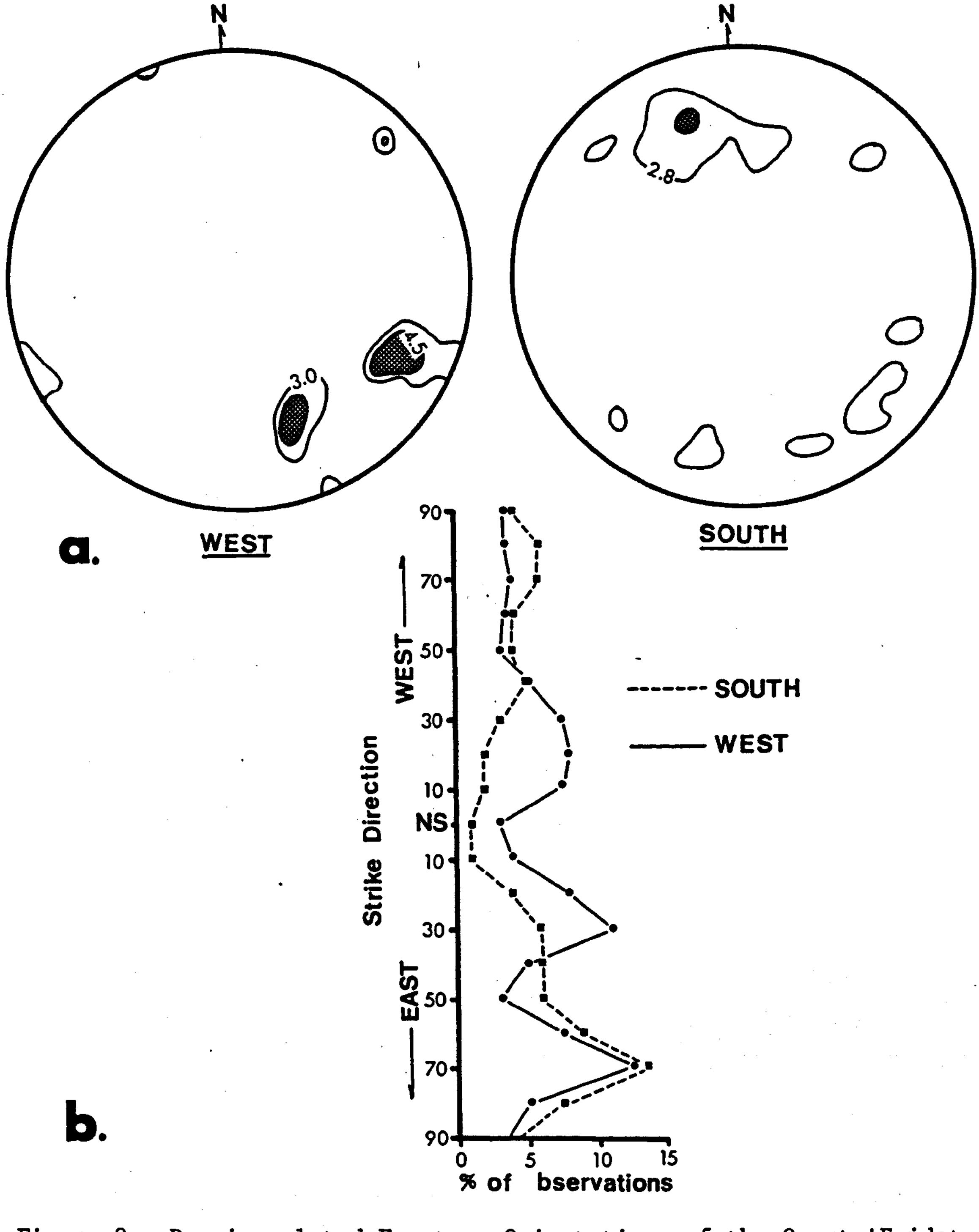

Figure 8. Domain-related Fracture Orientations of the Quartz+Epidote+K-feldspar Alteration Assemblage. --
(a) pi diagrams (b) strike histogram
West=200 points South=216 points
Contour interval is 1.5% for the West domain, with the 3.0% and 4.5% intervals shown. Contour interval for the South domain=2.8%. Contoured per 1% of area.

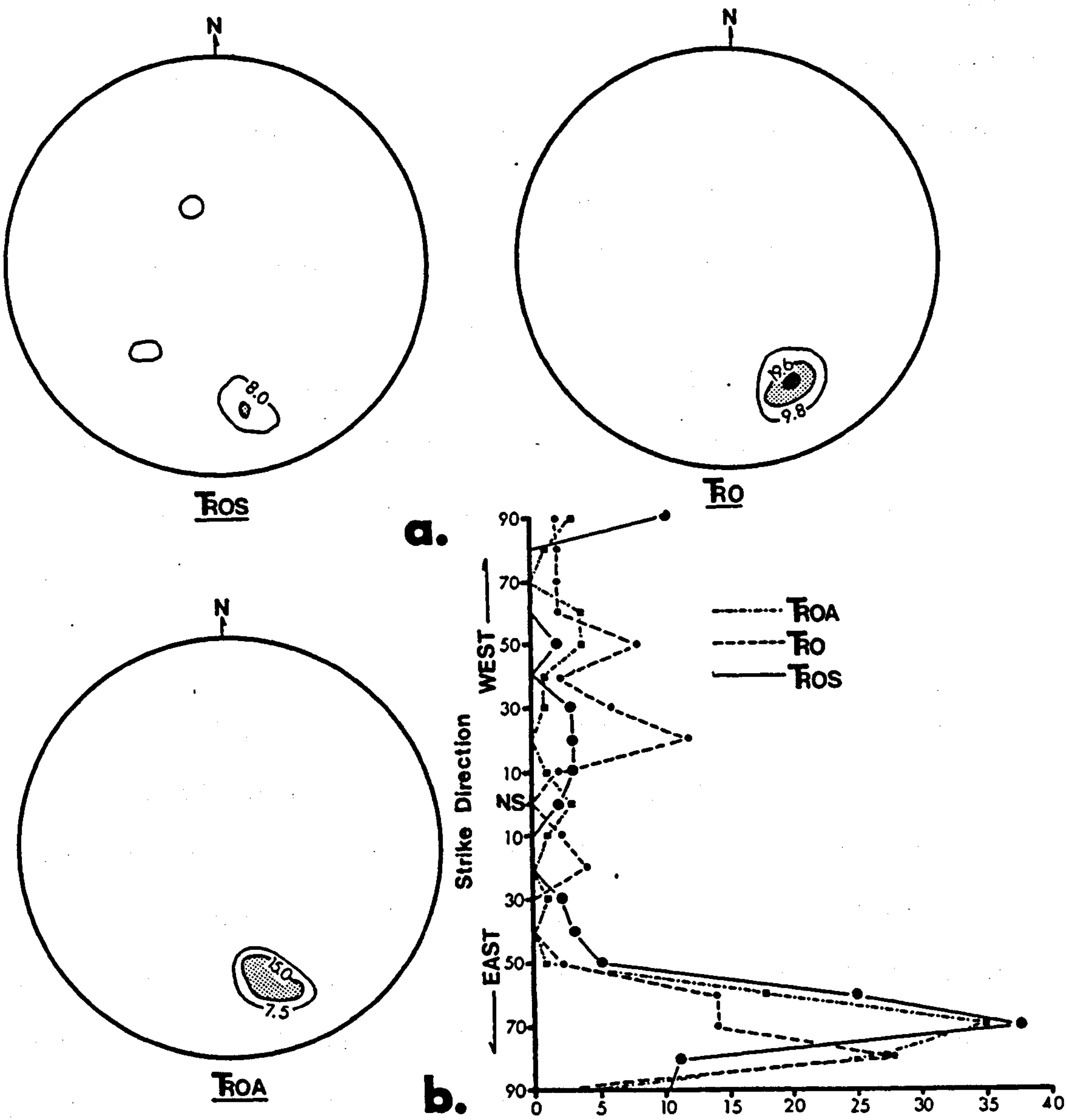

Figure 9. Rock Type-related Fracture Orientations of the Quartz+ Sulfide Alteration Assemblage.
(a) pi diagrams (b) strike histogram
Ŧoa=80 points Ŧos=49 points Ŧo=61 points
Contoured per 1% of area. Contour interval=7.5%, 8.0%, and 9.8% for Ŧoa, Ŧos, and Ŧo, respectively.

A plan-view map of dominant strike directions is especially effective in illustrating areal distributions of fracture orientations, as well as local differences in strike direction between the various alteration assemblages (Figure 10). The ENE trend, while persistent throughout the area, is especially dominant west-southwest of the quartz monzonite porphyry stock, where it is accompanied by NNW fracture strike directions in the nonsulfide assemblage. The NE trend becomes strikingly dominant southwest of the generator stock. Weakly expressed WNW-ESE fracturing is principally confined to the periphery of the observed nonsulfide and sulfide alteration assemblages.

Fracture Densities

The spatial relationship of fracture densities in the Ox Frame and Demetrie Volcanics to the Sierrita generator stock is presented by two methods: (1) fracture densities are plotted as a function of distance from a best-fit mineralizing center, located within the quartz monzonite porphyry stock (Figures 11 and 12), and; (2) plan-view maps illustrating "averaged" contoured fracture densities (Figures 13 and 14). The fracture density versus distance curves were constructed with points representing averaged fracture density values calculated at one-half kilometer intervals from the generator stock. Fracture density units on the vertical axis are given in inverse centimeters, with a density value of $0.02cm^{-1}$ reflecting

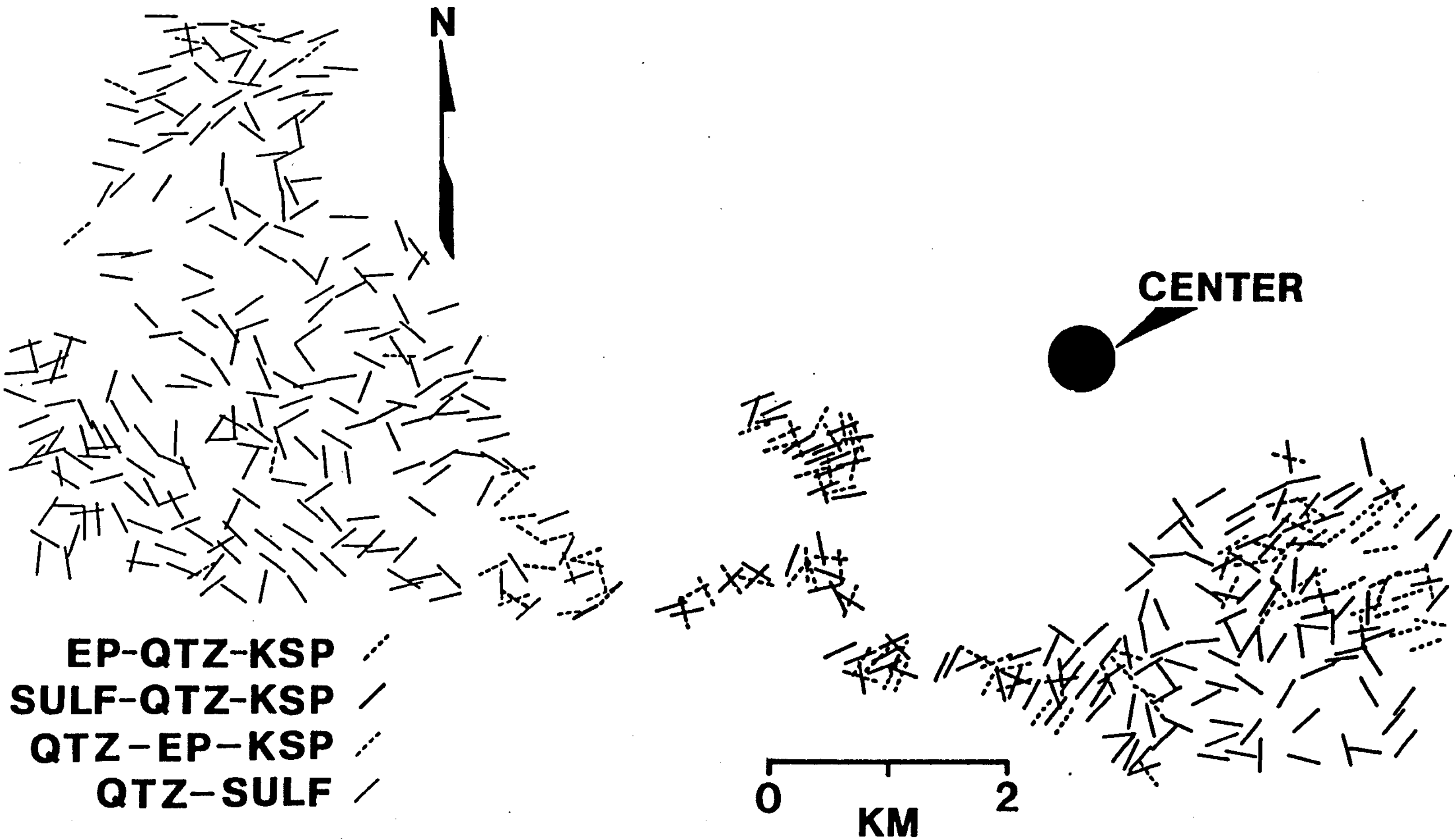

Figure 10. Plan Map of Dominant Fracture Strike Directions.

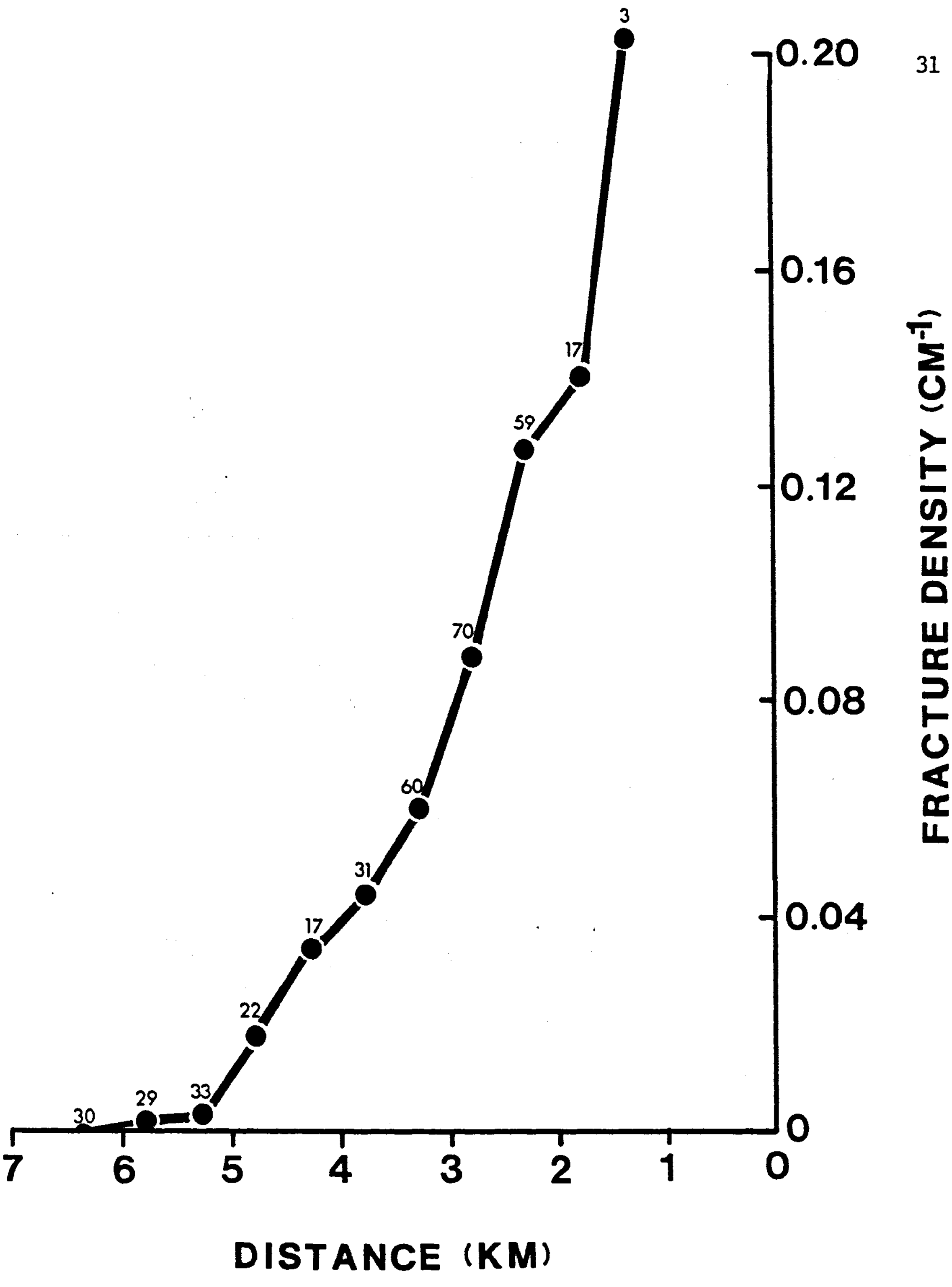

Figure 11. Integrated Fracture Density versus Distance Curve for the Sierrita-related Alteration Assemblages. -- The number above each data point is the number of stations in that interval.

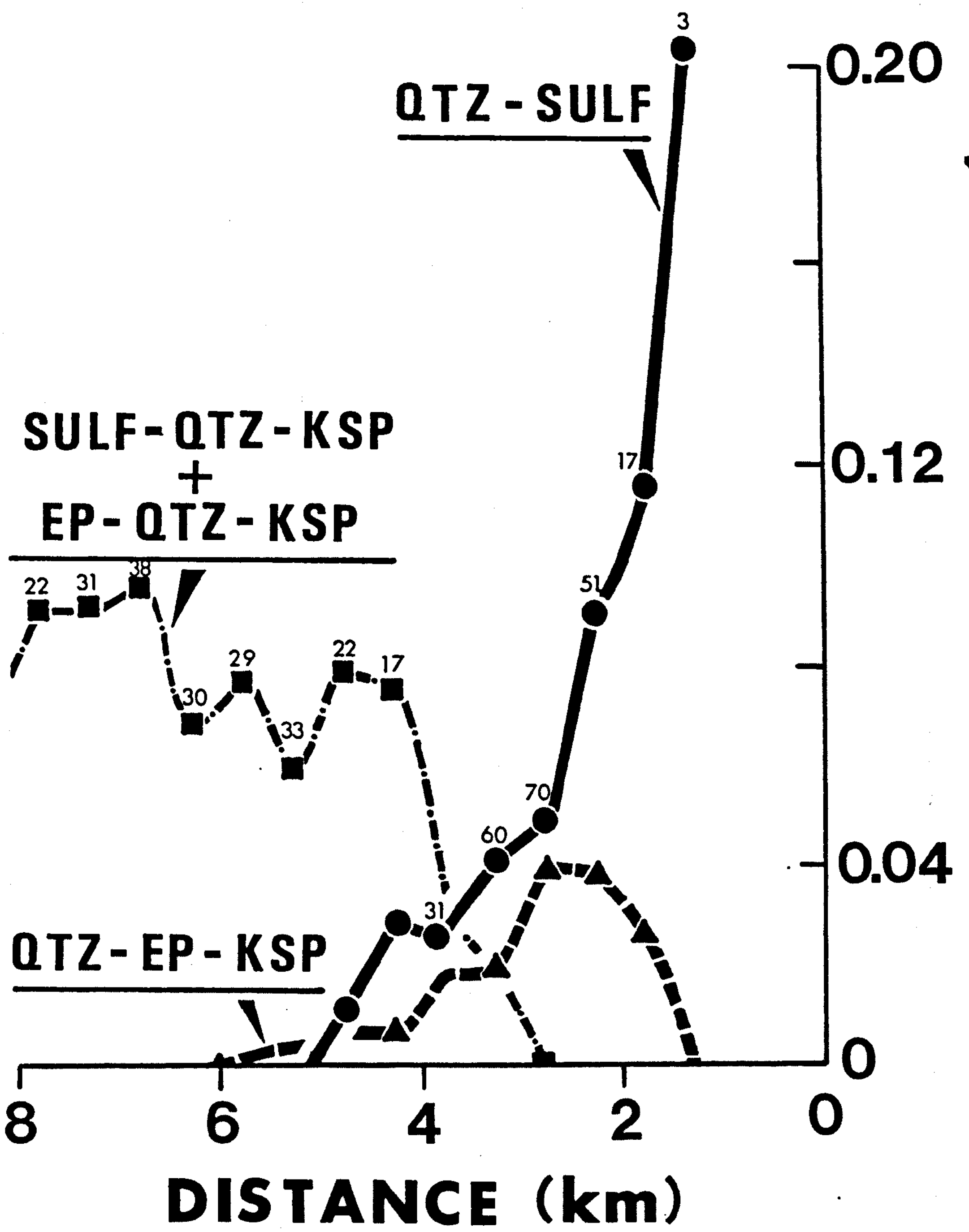

Figure 12. Fracture Density versus Distance Curves. -- The number above each data point is the number of stations in that interval.

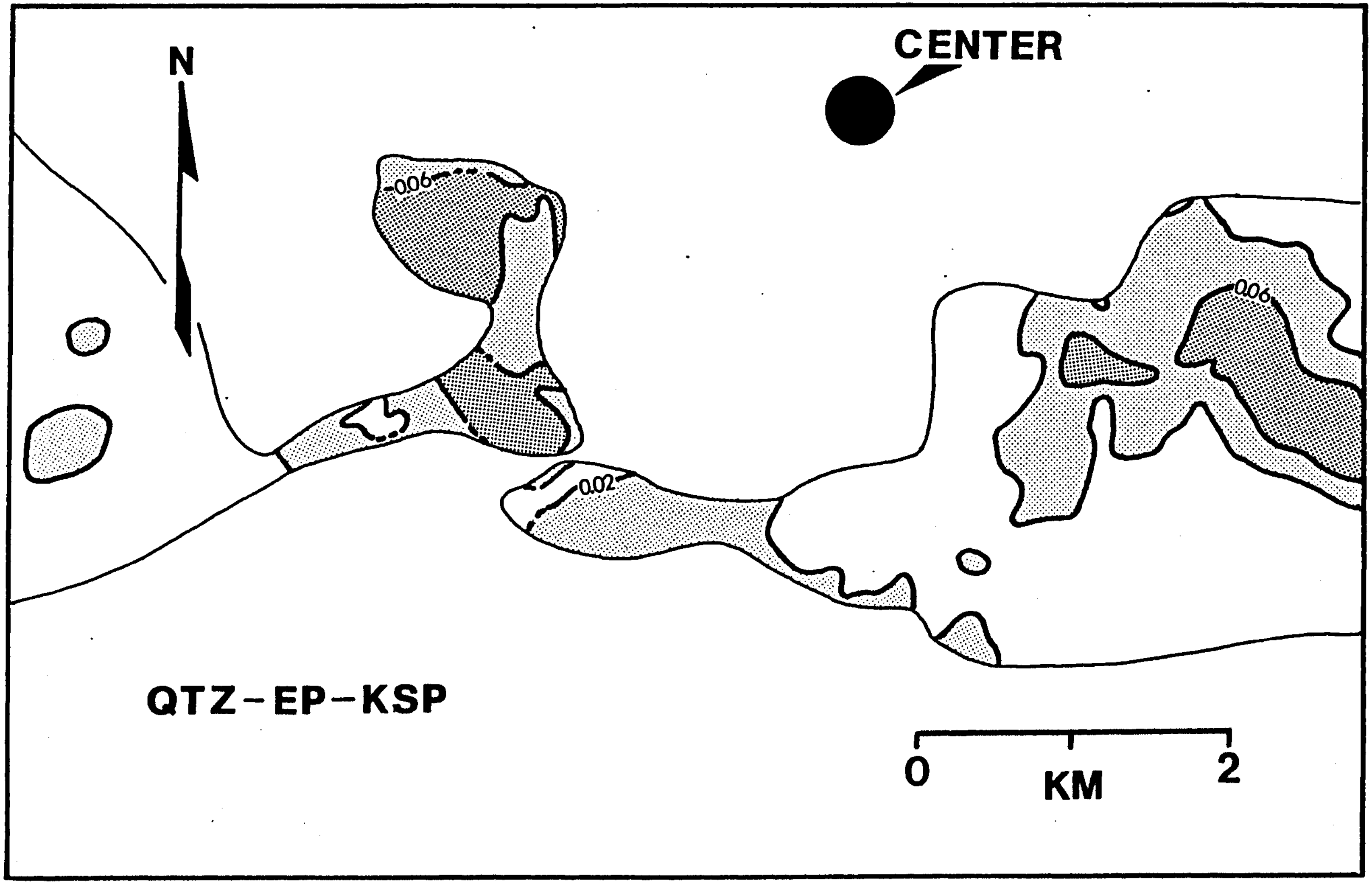

Figure 13. Fracture Density Contour Diagram for the Quartz+Epidote+K-feldspar Alteration Assemblage. -- Contour interval is 0.04cm^{-1}. Diagram includes the 0.02cm^{-1} and 0.06cm^{-1} intervals.

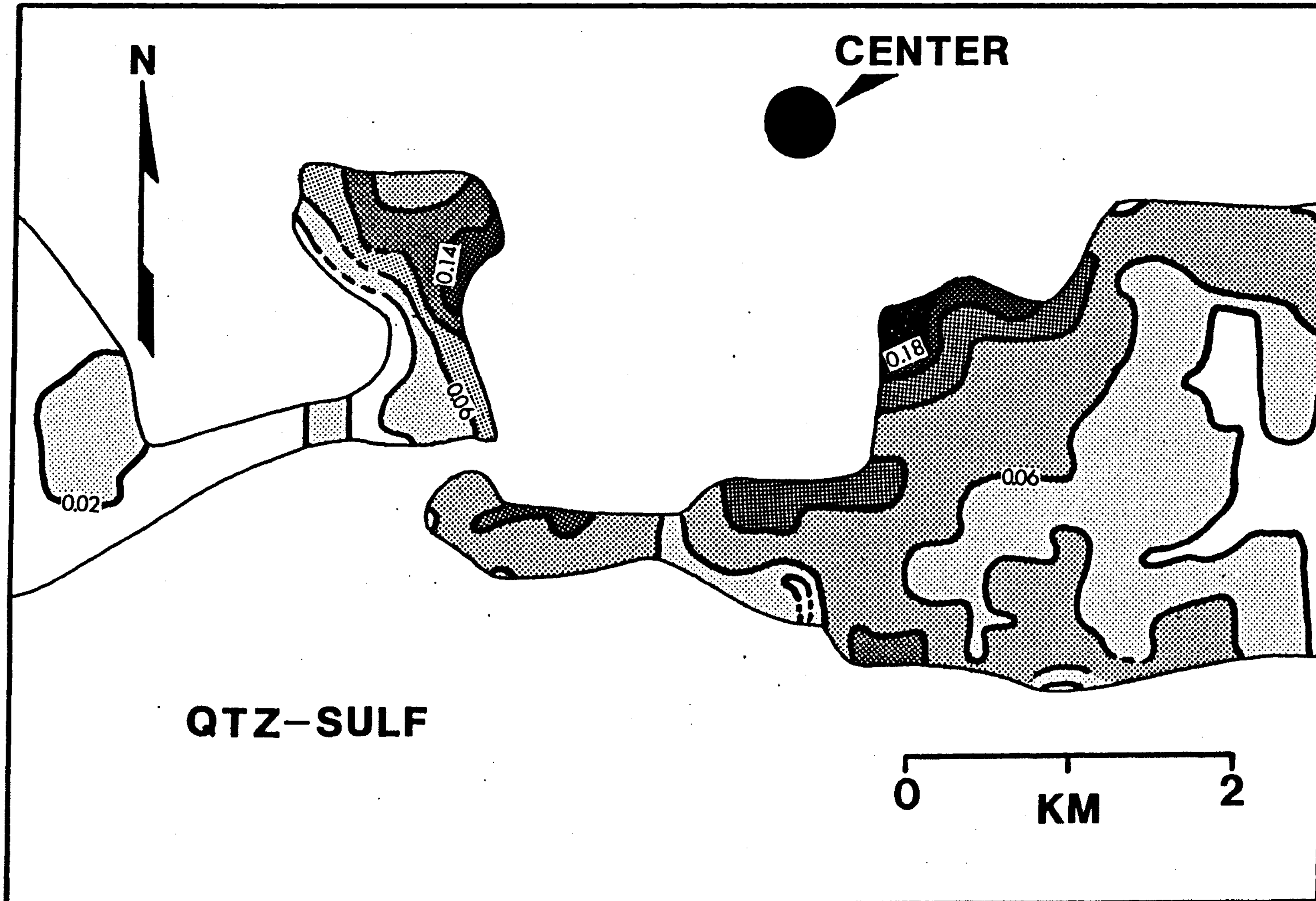

Figure 14. Fracture Density Contour Diagram for the Quartz+Sulfide Alteration Assemblage. -- Contour interval=0.04cm^{-1}. Diagram includes the 0.02cm^{-1}, 0.06cm^{-1}, 0.10cm^{-1}, 0.14cm^{-1}, 0.18cm^{-1}, and 0.22cm^{-1} intervals.

fractures spaced about one-half meter apart. Contouring fracture densities provides a graphic depiction of the areal distribution of individual fracture density values, allowing a more specific examination of the spatial relationship of fracturing to the proposed mineralizing center. "Averaged" contour fracture density diagrams were constructed by superimposing a scaled 200-meter orthogonal grid on a map of the study area and recording an average fracture density at each point center for an actual-area of 0.04 square kilometers. The final fracture density contour diagram is constructed about point centers representing station site averages for successively overlapping areas. These "averaged" contour diagrams are particularly effective in reducing local perturbations in fracturing and yet still retain enough resolution to ascertain the effects of structure and rock type. Mine dump material, extending about 1.5 kilometers south of the open pits, and the presence of post-mineralization Tertiary cover rocks within three to five kilometers south of the generator stock confines the study of Sierrita-related fracturing in the Mesozoic volcanic rocks, especially to the south.

The integrated fracture density curve for the entire study area indicates a drop in density values from a high of $0.20 cm^{-1}$ within 1.25 kilometers of the Sierrita center to the final disappearance of the Sierrita-related alteration assemblages at a distance of almost six kilometers (Figure 11). The integrated fracture density curve is a composite of the nonsulfide and sulfide assemblages.

Figure 12 summarizes the fracture density data for the quartz+epidote+K-feldspar and quartz+sulfide alteration assemblages and includes a composite curve for the two early assemblages.

The fracture density data generally depicts relatively widespread distribution of the nonsulfide assemblage, attaining moderate fracture densities that peak about 2.75 kilometers from the generator stock, with much higher densities displayed by the relatively areally restricted sulfide assemblage. The composite curve for the early epidote+quartz+K-feldspar and sulfide+quartz+K-feldspar assemblages indicates an abrupt appearance at about three kilometers, with fracture densities irregularly increasing westward, away from the quartz monzonite porphyry stock.

Both alteration assemblages eventually disappear with distance from the central stock, although their spatial patterns differ strikingly in detail (Figures 13 and 14). The erratic distribution of the quartz+epidote+K-feldspar assemblage is reflected by irregular fracture density contours (Figure 13). This pattern contrasts with the relatively regular contours of the later, quartz+sulfide alteration assemblage (Figure 14). Even at distances of 1.5 - 2.5 kilometers, fracture density gradients of this sulfide assemblage tend to focus on a mineralizing center located within the quartz monzonite porphyry stock at Sierrita.

Fracture Style: Straightness and Continuity

Straightness and continuity data are presented in three contexts: (1) fracture style as a function of rock type (Figure 15); (2) fracture style as a function of strike direction (Figure 16), and; (3) fracture style as a function of distance from the generator stock (Figure 17 and 18). The straightness and continuity values represented in these plots are based on the average of assigned values given to all fractures falling within a given measurement interval, whether that interval be distance, rock type, or strike direction. The rock type and fracture orientation comparisons are plotted with fracture style represented on the vertical axis by an average of the sum of straightness and continuity values. Fracture style as a function of distance from the central stock is plotted in a manner identical to that employed in fracture density versus distance plots, with the straightness and continuity curves based on points representing fractures from many stations, averaged at one-half kilometer intervals.

Fracture style data are summarized in Figures 15 through 18. Fracture styles of both the quartz+epidote+K-feldspar and quartz+sulfide alteration assemblages increase in straightness and continuity from a low in the poorly-welded tuff of the upper rhyolitic member of the Demetrie Volcanics to a high in the quartzites of the Ox Frame Volcanics. Specifically, an increasing order of fracture style

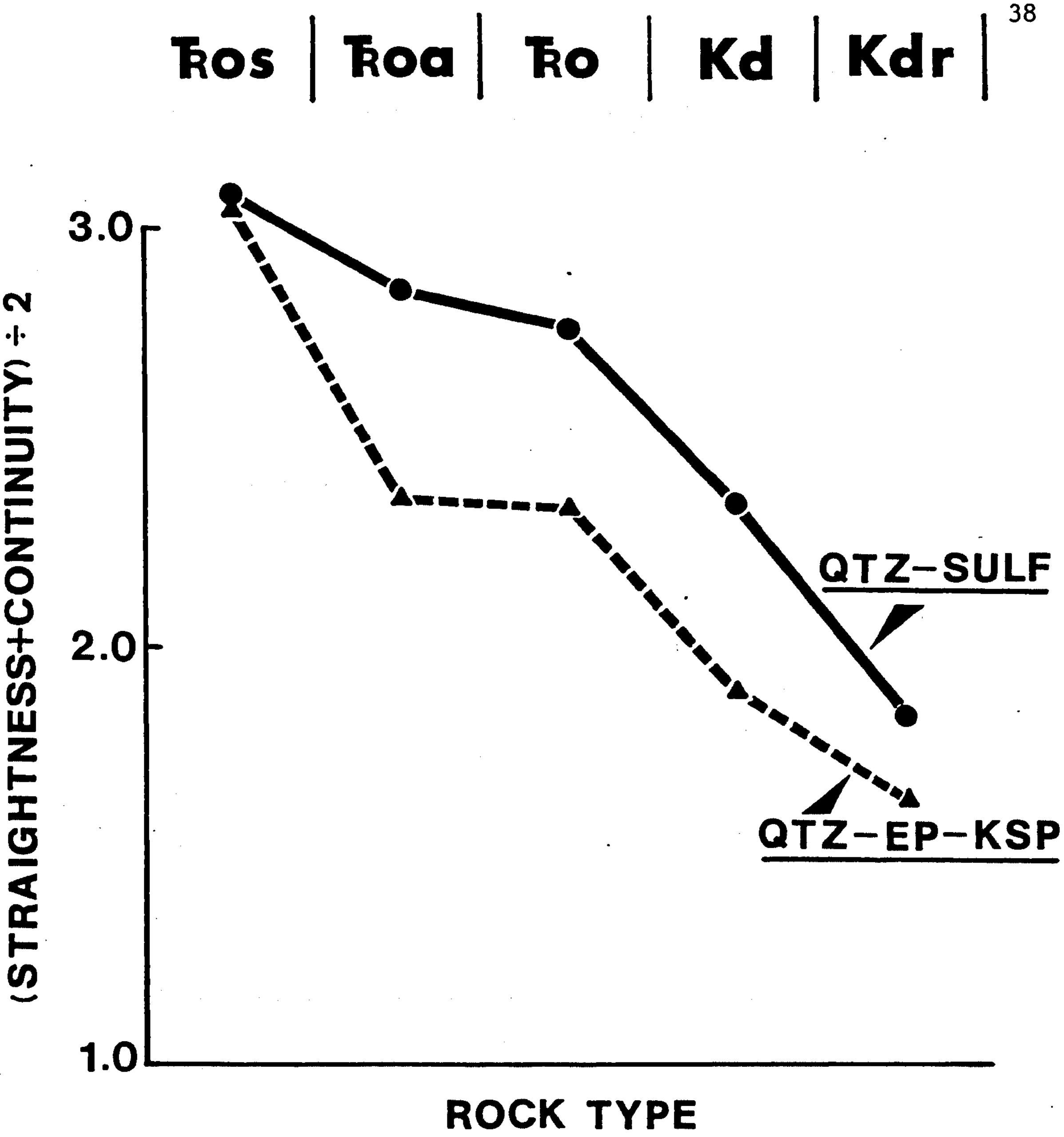

Figure 15. Straightness and Continuity versus Rock Type.

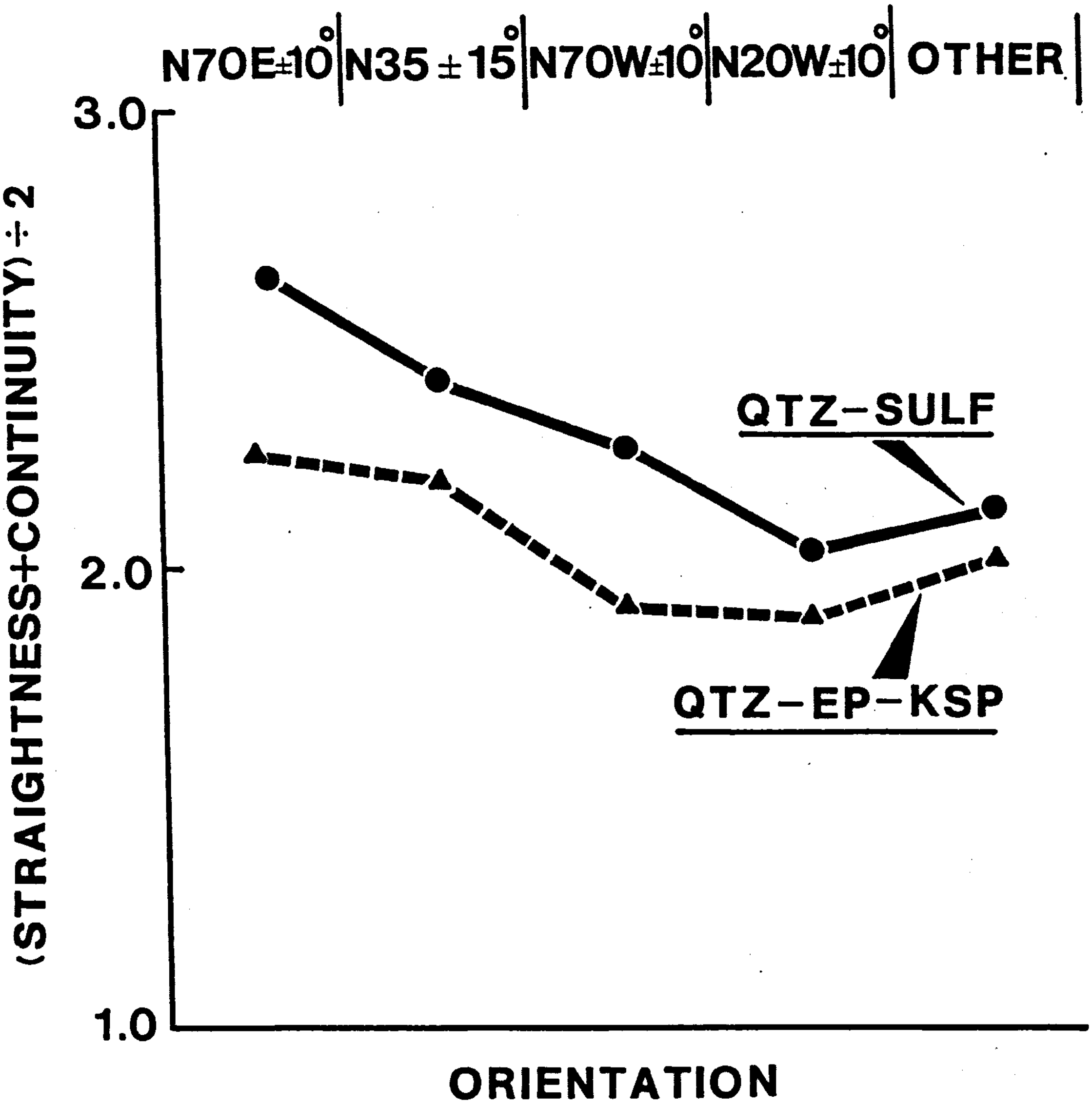

Figure 16. Straightness and Continuity versus Orientation for the Sierrita-related Alteration Assemblages.

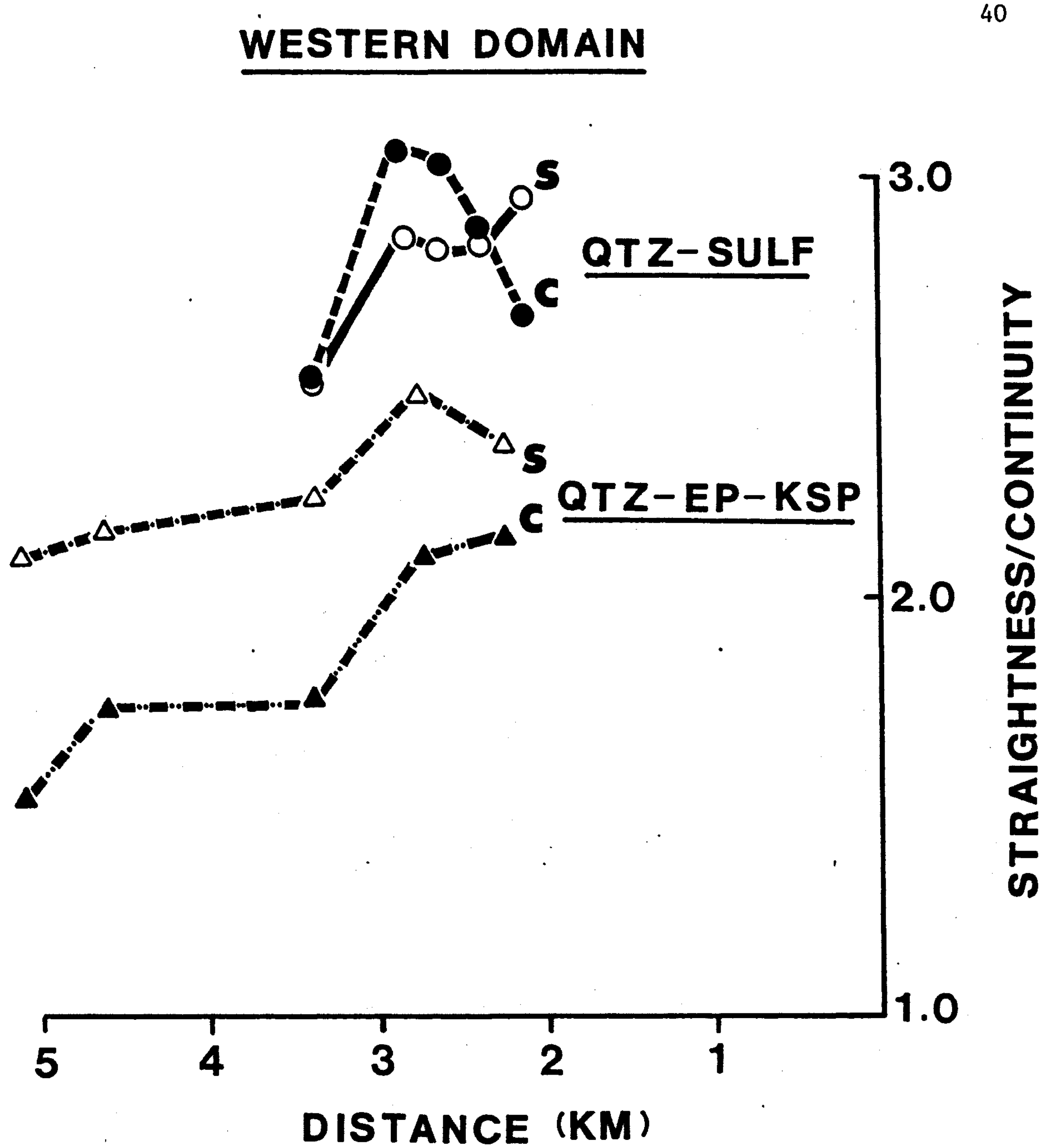

Figure 17. Straightness and Continuity versus Distance for the Sierrita-related Alteration Assemblages in the Western Domain. -- S=straightness, C=continuity.

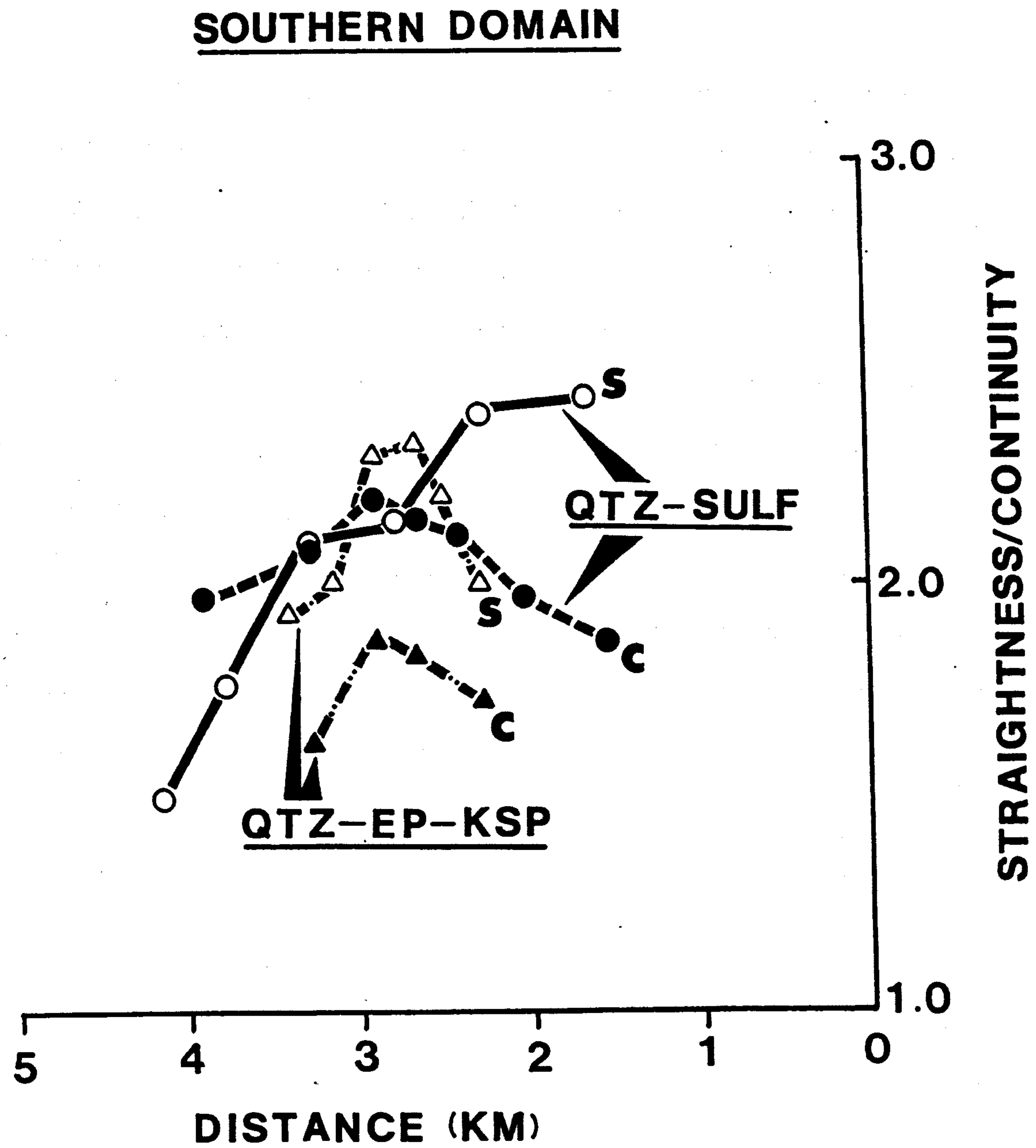

Figure 18. Straightness and Continuity versus Distance for the Sierrita-related Alteration Assemblages in the Southern Domain. -- S=straightness, C=continuity.

values is indicated for a Demetrie rhyolite-Demetrie andesite-Ox Frame rhyolite-Ox Frame andesite-Ox Frame quartzite sequence. Figure 15 also reveals higher straightness and continuity values among fractures of the sulfide assemblage than the earlier, non-sulfide assemblage. Fracture style values are generally higher among fractures with strike directions reflecting fracture orientation maxima, especially the ENE regional trend (Figure 16). Fracture style plotted as a function of distance (Figure 17 and 18) has been divided into lithologically distinct western and southern domains because of the effect of rock type on straightness and continuity. These eight curves are united by an abrupt decrease in fracture style values at a distance of about three kilometers from the Sierrita center.

Chapter 7

DISCUSSION OF FRACTURING SPATIALLY ASSOCIATED WITH THE SIERRITA GENERATOR STOCK

Lithologic Influence on Fracture Formation

Lithologic influences on the formation of the quartz+epidote+K-feldspar and quartz+sulfide fracture-controlled alteration assemblages are relatively minor. Fracture orientation maxima, while varying somewhat in intensity in the western and southern domains, are consistent among the various rock types. The rhyolitic members of the Demetrie Volcanics are the only rock types obviously associated with anomalous fracture densities. Outcrops of the bedded and poorly-welded ash-flow tuff of the upper rhyolitic member, located south and west of the mine dumps, correspond to general fracture density contour lows for both alteration assemblages. The resistant lower ash-flow tuff in the northeast corner of the study area appears to correspond to a general fracture density low for the nonsulfide assemblage and a slight fracture density high for the sulfide assemblage. The strongest lithologic influences on fracture formation appear to have been on the mineralogy of fracture-controlled alteration assemblages, with a general correlation between an increase in the relative abundance of epidote and chlorite in the more basic rock types (Table 1), and on fracture style, with both alteration assemblages following similar trends among the five principal rock types (Figure 15). Fractures in the erosionally resistant rocks of the Ox Frame Volcanics, and especially the hill-capping quartzites, are generally straighter and more continuous than fractures in the Demetrie Volcanics, a unit that forms a recessive topography.

Influence of Faults on Fracture Formation

Faults appear to have affected fracture densities of both alteration assemblages. A N50W-trending fracture density high in the western half of the study area (Figure 13) is centered precisely over a similarly oriented fault. NE-trending density contours of the sulfide assemblage at the southeastern edge of the study area are distributed along a fault and its walls (Figure 14). The reappearance of this quartz+sulfide assemblage about 4.25 kilometers west of the generator stock corresponds to two ENE-trending faults in this vicinity. These perturbations in fracture density contours occur near the areal limits of the sulfide assemblage. Fracture density gradients near the Sierrita porphyry system are strongly centered on the quartz monzonite porphyry stock. With increasing distance from the center, and subsequently lower fracture densities, the contours become more irregular, perhaps reflecting an increased structural influence on fracture distribution as suggested by fracture density contour deflections about faults.

Fracture Style

The preponderance of fractures throughout the study area are traceable for 1.5 - 3.0 meters, display minor strike irregularities, and have been categorized into straightness and continuity values of 2 or 3. Variations in values of the fracture style versus distance plots of Figures 17 and 18 reflect changes in the relative abundances of fractures deviating from the normal fracture mode. The abrupt decrease in fracture style values which occurs at about 3.0 - 3.25 kilometers from the Sierrita mineralizing center is consistent for both alteration assemblages throughout the study area and reflects an increase in the abundance of irregular, discontinuous fractures peripheral to the high density fracturing closely associated with the generator stock. With the exception of the high order fracture straightness of veins containing the sulfide assemblage, the fracture style curves indicate a slight increase in the relative abundance of irregular, discontinuous fractures close to the center of the system.

The straightness and continuity curves (Figures 15, 16, 17, and 18) can be interpreted in terms of general fracture style distribution patterns.

1. The preponderance of fractures in the Mesozoic volcanic rocks are traceable for 1.5 - 3.0 meters and display minor strike irregularities along their length.

2. Fractures of the sulfide alteration assemblage are generally straighter and more continuous than those of the earlier, nonsulfide assemblage.

3. Fracture style values are higher for fractures in the Ox Frame Volcanics, composed of resistant rocks, than in the Demetrie Volcancis, which forms a recessive topography.

4. Regional stresses apparently exerted some influence over fracture style, with ENE- and NE-striking fractures generally being straighter and more continuous than dissimilarly oriented fractures.

5. Irregular, discontinuous fractures controlling both alteration assemblages increase in relative abundance in the periphery of the Sierrita system over three kilometers from the quartz monzonite porphyry stock. Irregular, discontinuous fractures apparently also increase in abundance toward the mineralizing center at distances less than 2.75 kilometers for the nonsulfide assemblage. It should be emphasized that the study area only encroaches within about 1.5 kilometers of the generator stock.

6. Poor vein preservation precludes consistent documentation of vein widths. However, the quartz+sulfide veins were narrow, usually less than two or three millimeters in width. The quartz+epidote+K-feldspar assemblage is distinguished by commonly demonstrating highly variable vein widths.

All eight fracture style curves plotted as a function of distance from the Sierrita center are united by an abrupt decrease in straightness and continuity at about 3.0 - 3.25 kilometers from the progenitor stock. This 3.0 kilometer distance marks the approximate limit of intense fracturing related to a Sierrita center, not only in the Mesozlic volcanic rocks, but to the west and north as well, in the Harris Ranch Quartz Monzonite and Ruby Star Granodiorite. Results of the present study reveal that the third alteration assemblage reaches a peak in fracture density at about 2.75 kilometers from the mineralizing center, followed by a continuous decline with increasing distance. The sulfide assemblage drops rapidly in fracture density away from the generator stock, with the three kilometer distance marking the approximate beginning of a final gradual diminishment in density (Figure 12). In the Ruby Star Granodiorite, northwest of the Sierrita open pit, high sulfide assemblage fracture densities are confined to areas within three kilometers of the generator stock (Haynes and Titley, 1980). Northeast of the Esperanza open pit, Manske (1980) defines a "boulder line" in the Ruby Star Granodiorite at an average of three kilometers from the quartz monzonite porphyry stock, marking the decline in fracture density to "background" values. White (Appendix A, 1980) notes an abrupt decline in fracture density for the sulfide assemblages in the Harris Ranch Quartz Monzonite west of the Sierrita open pit, occurring at an average of 3.25 kilometers from the center at Sierrita. It is apparent that the limit of intense fracturing related to the Sierrita generator stock generally occurs at a distance of about three kilometers, and is reflected in fracture style by an abrupt increase in the relative abundance of irregular, discontinuous fractures.

Strain

The distribution and orientation of fractures in the vicinity of the Sierrita porphyry copper deposit prompt some general speculations concerning the implications of strain in the study area. The probable dominant strain reflected by fractures and veins is one of simple dilation. Vein apertures are variable, but generally less than five millimeters wide. A fracture density of $0.10cm^{-1}$, reflecting fractures spaced about 10 centimeters apart, therefore implies a volume increase of almost 1% for an assumed average vein width of one millimeter. Vein offsets and slickensides are evidence of slip along fractures, suggesting a distortional strain component. Vein preservation is only rarely sufficient for measuring relative offset, although some ENE-trending veins of the sulfide assemblage have offset nonsulfide veins with a left-separation motion. The strain implications of fracture straightness and continuity are not presently understood. However, it appears reasonable to suggest that fracture density is a general reflection of the amount of strain represented by fracturing. Dilational strain is probably greatest normal to an ENE-trend, the predominant fracture orientation in the study area.

Evolution of Fractures

Two fracture-controlled alteration assemblages are present in the Mesozoic volcanic rocks south of the Sierrita porphyry copper system that display spatial distribution patterns in fracture density related to the quartz monzonite porphyry stock at Sierrita. Fractures controlling an early, quartz+epidote+K-feldspar assemblage attained moderate densities and relatively widespread, although irregular areal distribution. This early hydrothermal event was succeeded by an episode that produced a quartz+sulfide assemblage related to high density, but relatively areally restricted veins displaying fracture density gradients centered on the generator stock. Both vein types are dominated by an orientation maximum of N70E $\pm$ 10^{o}, with a pronounced NE trend. Weakly developed WNW and NNW fracture orientation trends are also present. Fracture style curves indicate that fracturing in the distal regions of the Sierrita system is marked by a relative abundance of irregular, discontinuous fractures.

The localization of dense fracturing and alteration about the quartz monzonite porphyry body suggests that fracture formation was strongly influenced by the emplacement and crystallization of this stock. The ENE fracture orientation maximum, noted in Laramide-age intrusive rocks throughout Arizona (Rehrig and Heidrick, 1976; Heidrick and Titley, in press) emphasizes the important role of regional stresses in fracture formation. The evolution of fractures in the Mesozoic volcanic rocks south of the Sierrita system, and the final fracture geometry, appear to have been controlled by the combined effects of an intrusion center interacting with regional-tectonic stresses.

Chapter 8

AN EARLY HYDROTHERMAL EVENT

Fracture distribution, distinctive alteration mineralogy and fracture orientations, and fluid inclusion data (White, 1980) suggest that the first alteration assemblage, epidote±quartz± chlorite vein filling with a selective K-feldspar±chlorite halo, and the second alteration assemblage, sulfide±quartz±K-feldspar±epidote± chlorite vein filling occassionally with a selective ±K-feldspar± quartz halo, constitute a distinct, early hydrothermal event not obviously associated with the generator stock of the Sierrita porphyry copper system. The principles derived from the study of Sierrita-related fracturing have been applied to this early hydrothermal system in an attempt to locate a possible source.

Fracture Orientations

Fracture orientation data for the two early alteration assemblages indicate an ENE maximum with relatively minor WNW and NNE peaks of the epidote+quartz+K-feldspar assemblage, contrasting with more diffusely oriented fracturing for the later sulfide+quartz+ K-feldspar assemblage, which has weakly defined ENE and NNW fracture orientation maxima visible on the contoured pi diagram (Figure 19).

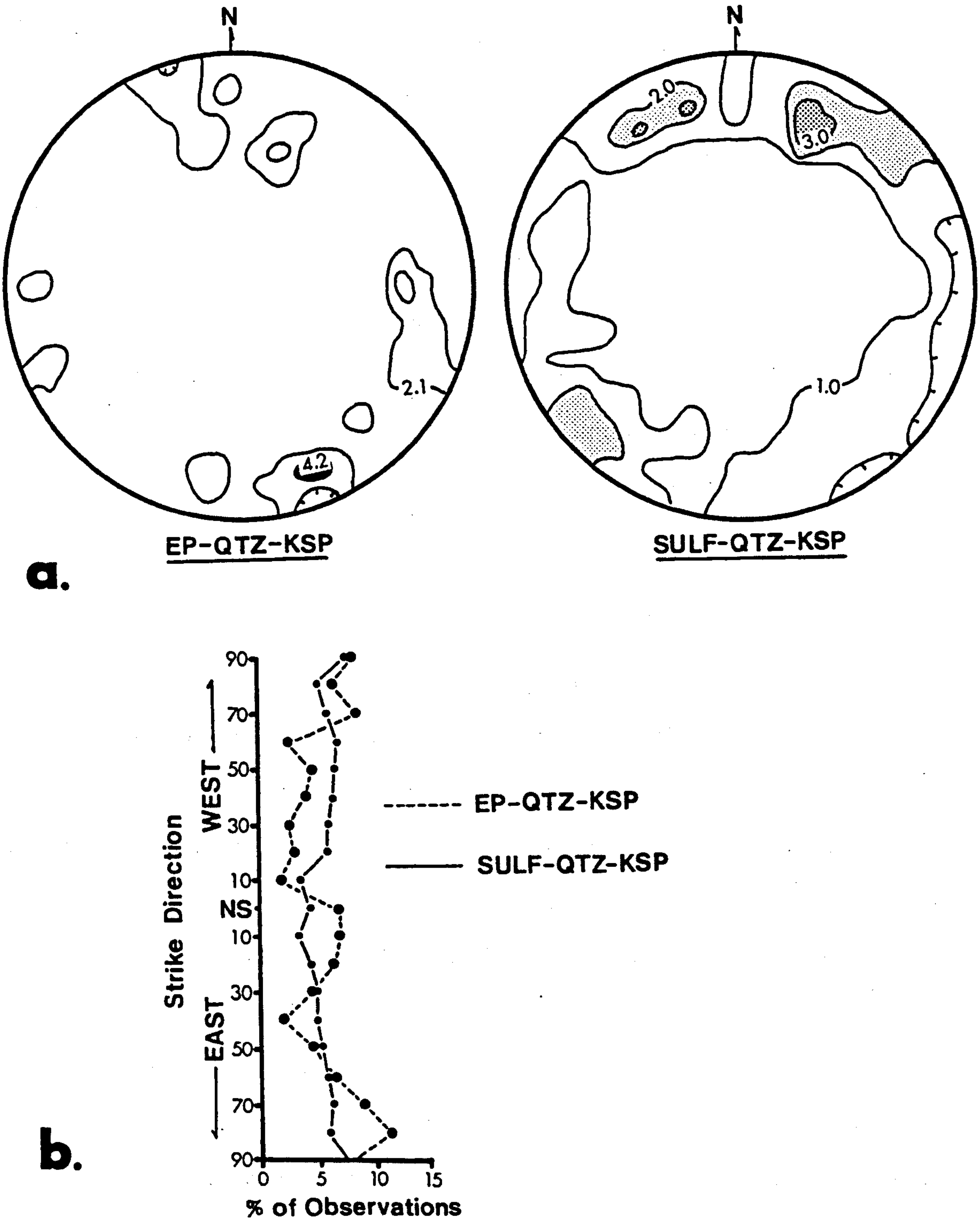

Figure 19. Fracture Orientations for the Epidote+Quartz+K-feldspar and Sulfide+Quartz+K-feldspar Alteration Assemblages. -- (a) pi diagrams, (b) strike histogram
Ep-Qtz-Ksp=191 points Sulf-Qtz-Ksp=1226 points.
Contoured per 1% of area. Contour interval=2.1% and 1.0% for the Ep-Qtz-Ksp and Sulf-Qtz-Ksp assemblages, respectively.

However, orientations of the sulfide assemblage in the Red Boy Rhyolite are resolved into well-defined maxima reflecting regional trends (Figure 20). Over 20% of measured fracture strike directions for this rock type fall into ENE double maxima of N60E $\pm$ 5° and N80E $\pm$ 5°. These ENE double orientation maxima have been documented in and near Laramide-age intrusive rocks throughout Arizona (Heidrick and Titley, in press). The Red Boy Rhyolite also displays lesser WNW and N30W $\pm$ 10° orientation maxima reflecting regional trends (Rehrig and Heidrick, 1972). Figure 10 summarizes the spatial distribution of prominant fracture strike directions calculated at each field station site.

Fracture Densities

Fracture density contour diagrams for the two early alteration assemblages reveal spatial distributions situated well west of the Sierrita porphyry copper deposit. The eastern edge of the area shown in Figures 21 and 22 is over 2.5 kilometers west of the quartz monzonite porphyry stock. The epidote+quartz+K-feldspar assemblage occurs in a broad NW-trending belt, with moderate to low fracture densities (Figure 21). This assemblage exhibits an erratic distribution, with the faint suggestion of a NE cross-trend to the principal NW-SE distribution pattern. Fracture density contours for the sulfide+quartz+K-feldspar assemblage indicate higher fracture densities, with

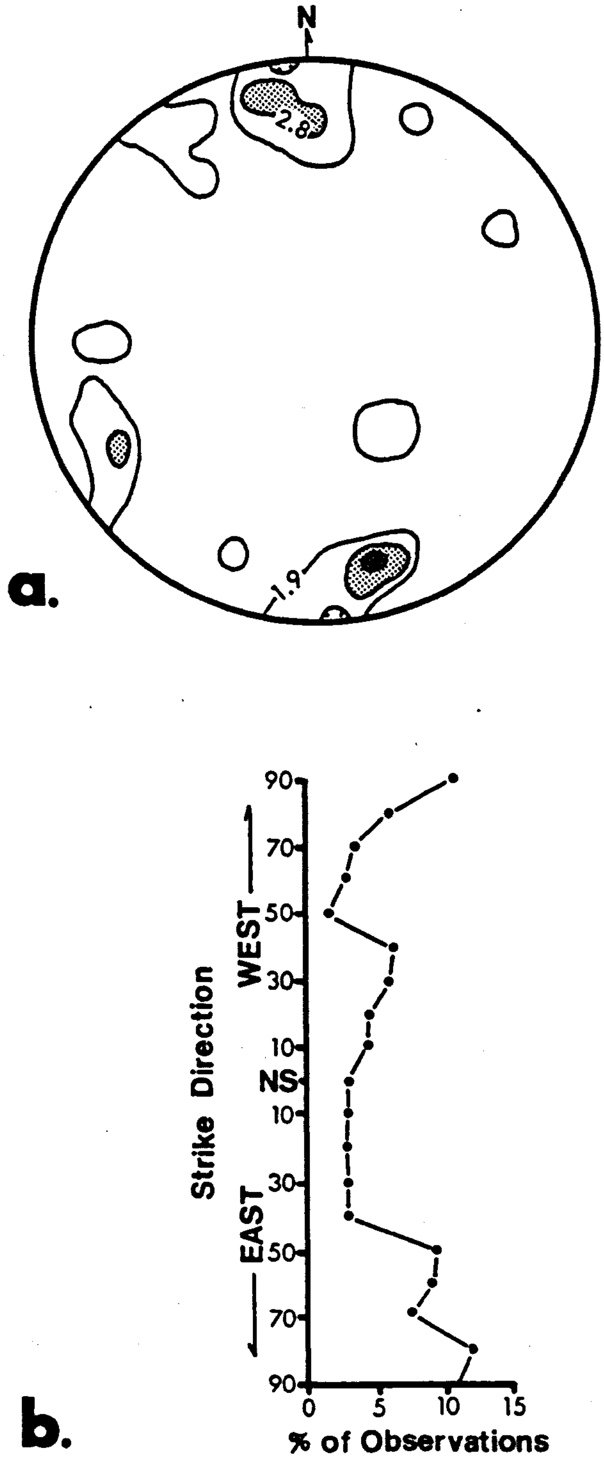

Figure 20. Fracture Orientations of the Sulfide+Quartz+K-feldspar Alteration Assemblage in the Red Boy Rhyolite. -- (a) pi diagram; (b) strike histogram. Based on 216 points. Contoured per 1% of area. Contour interval=1.9%.

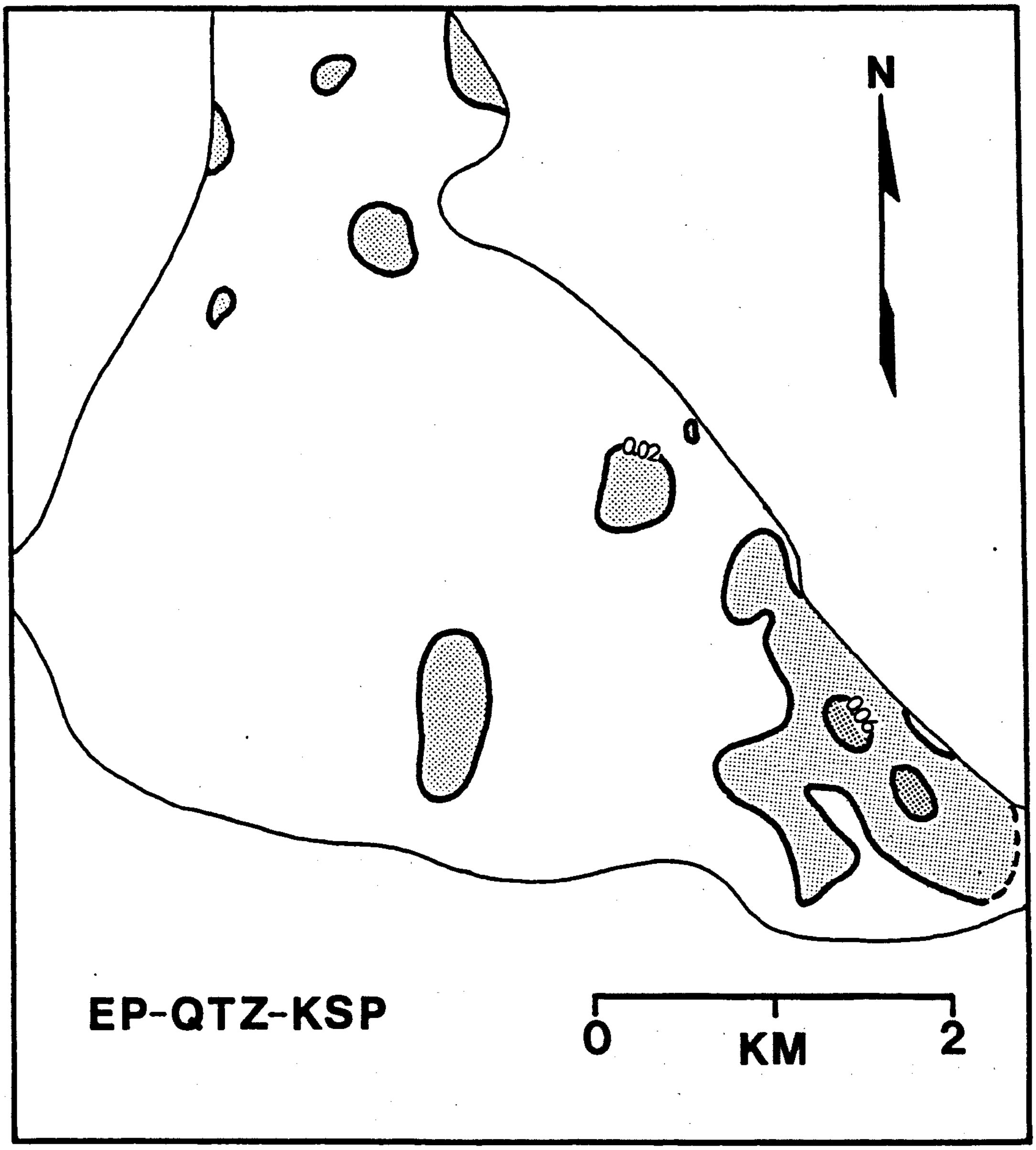

Figure 21. Fracture Density Contour Diagram for the Epidote+Quartz$\pm$K-feldspar Alteration Assemblage. Contour interval= $0.04 cm^{-1}$. Diagram includes the $0.02 cm^{-1}$ and $0.06 cm^{-1}$ intervals.

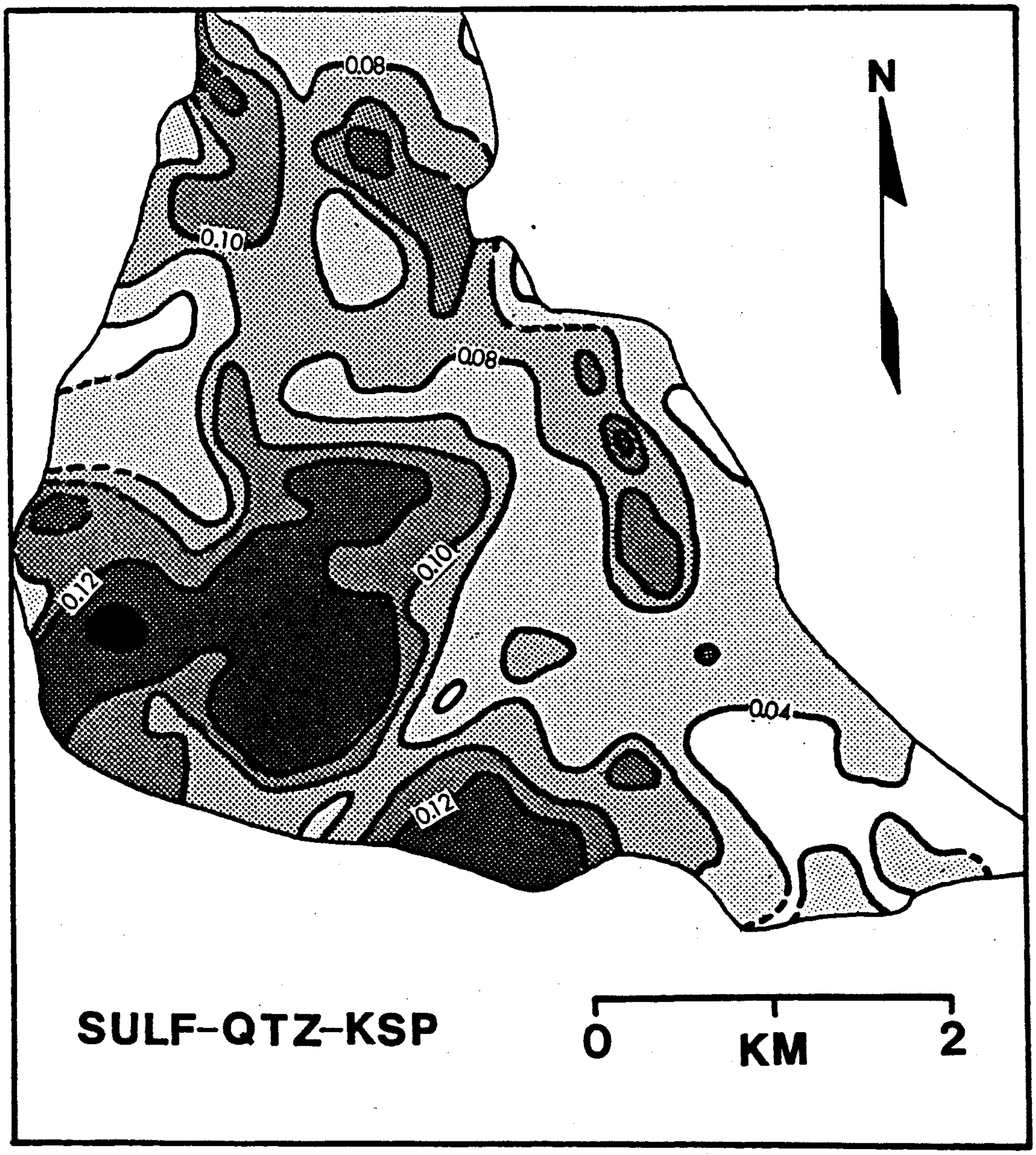

Figure 22. Fracture Density Contour Diagram for the Sulfide+Quartz+K-feldspar Alteration Assemblage. -- Contour interval generally=0.04cm^{-1}. Diagram includes the 0.04cm^{-1}, 0.08cm^{-1}, 0.10cm^{-1}, 0.12cm^{-1}, and 0.16cm^{-1} intervals. The 0.10cm^{-1} contour interval is included to help elucidate certain features described in the text.

a relatively regular distribution (Figure 22). Three features displayed by this fracture density contour diagram suggest a fracturing center focused in the southwest corner of the study area.

1. The highest fracture density contours are located at the proposed center, with a general drop in fracture densities away from this area.
2. Fracture density gradients appear to bend around an ENE-trending axis that intersects the fracture density maximum.
3. A concentric band of high fracture density contours lies precisely along a circular arc with a 2.75 kilometer radius whose origin is at the fracturing epicenter.

Figure 23 summarizes the fracture density data plotted as a function of distance from the center of highest fracture densities. The first, nonsulfide assemblage is absent near the center and maintains low fracture densities until about 3.5 kilometers, where it peaks and then disappears at a distance of about 5.5 kilometers. A general decrease in fracture densities from a high at the center to a final disappearance at a distance of about five kilometers characterizes the sulfide assemblage. The fracture density peak positioned at 2.75 kilometers from the origin corresponds to the concentric arc of high density contours observed in Figure 22.

Fracture Style

Figures 24 and 25 summarize the fracture style data for the first two alteration assemblages. Fractures with orientations

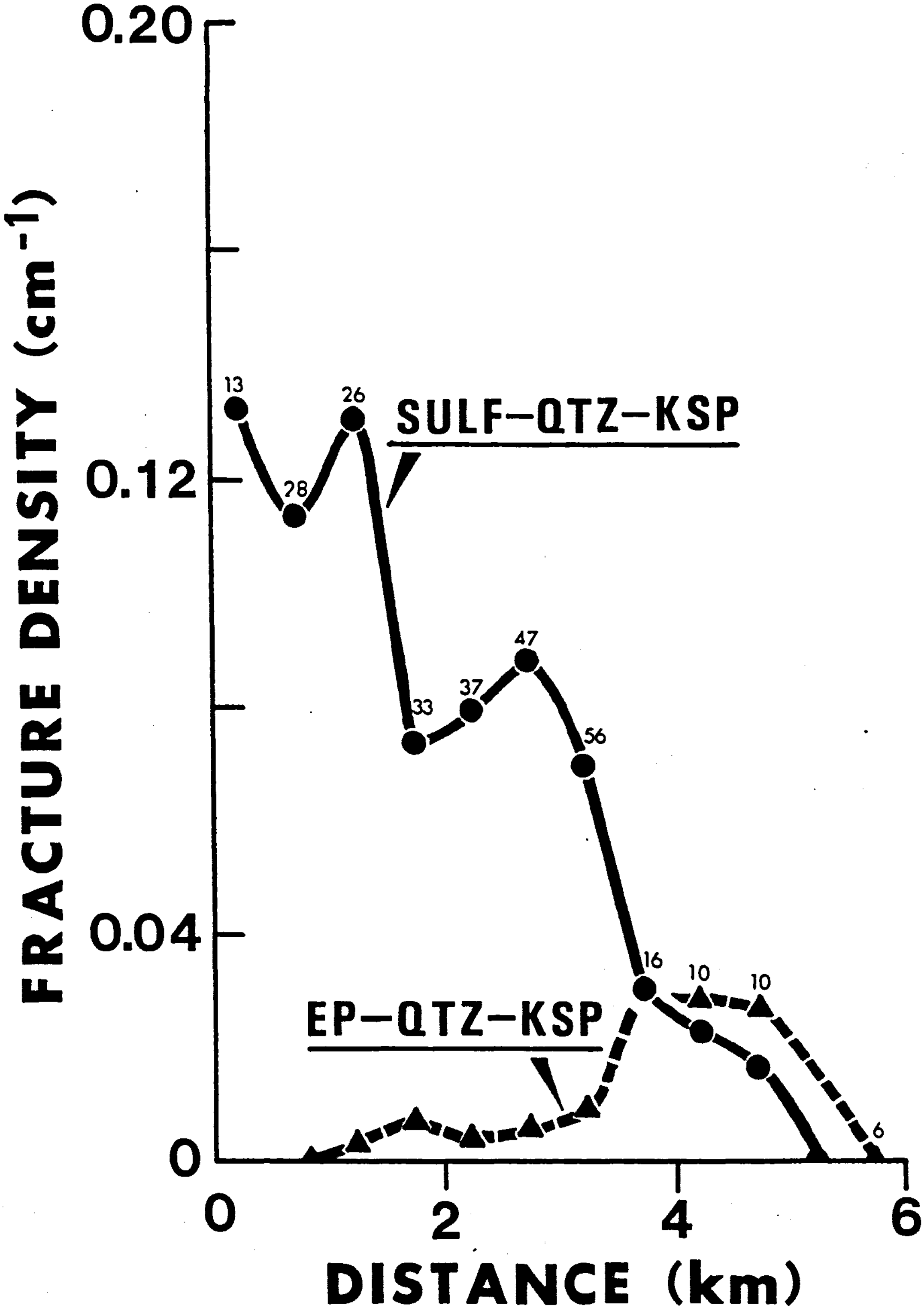

Figure 23. Fracture Density versus Distance for the Epidote+Quartz+K-feldspar and Sulfide+Quartz+K-feldspar Alteration Assemblages. -- Origin corresponds to the fracturing epicenter described in text. Numbers above data points represent the number of stations in each interval.

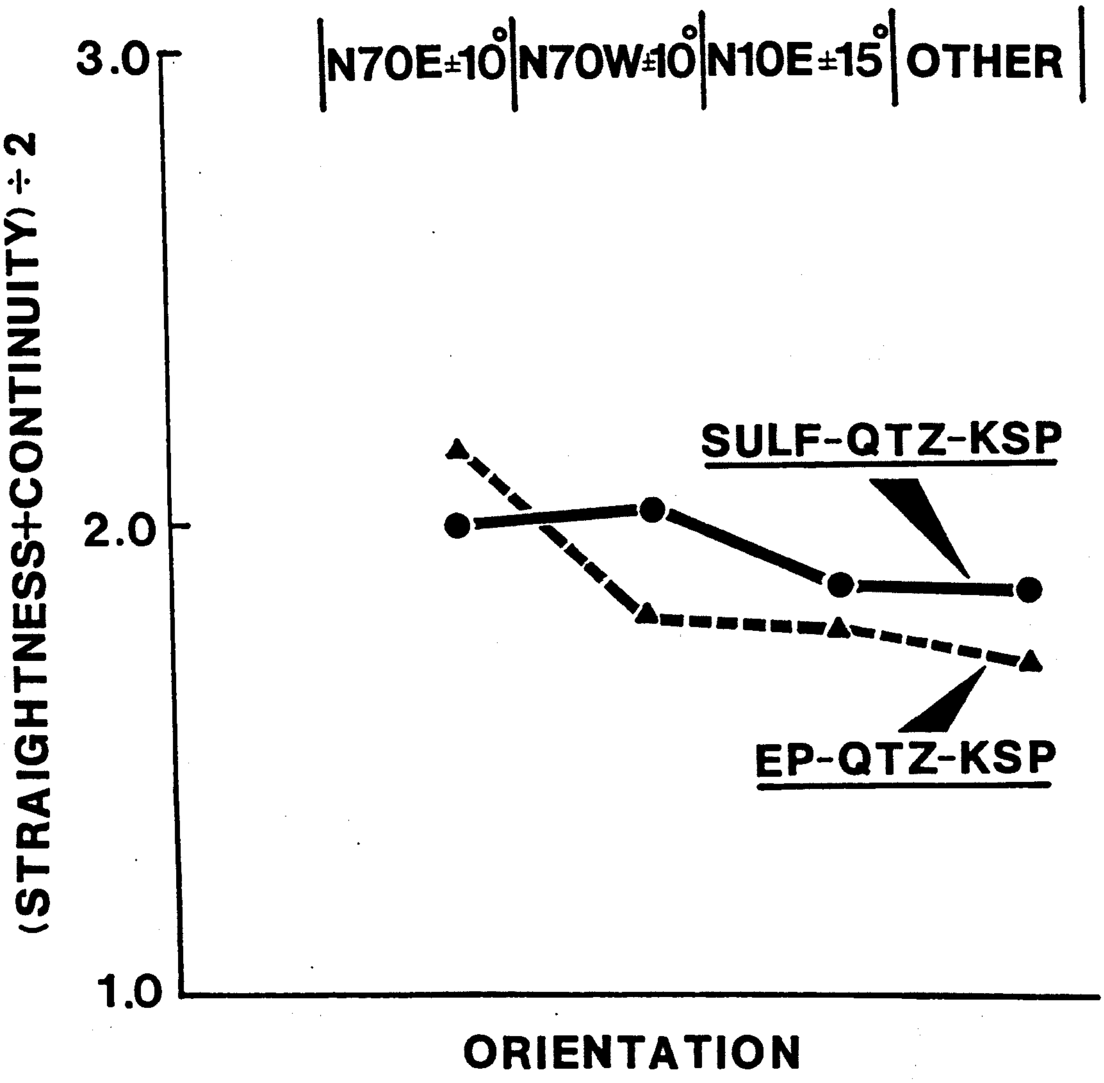

Figure 24. Straightness and Continuity versus Orientation for the Early Alteration Assemblages.

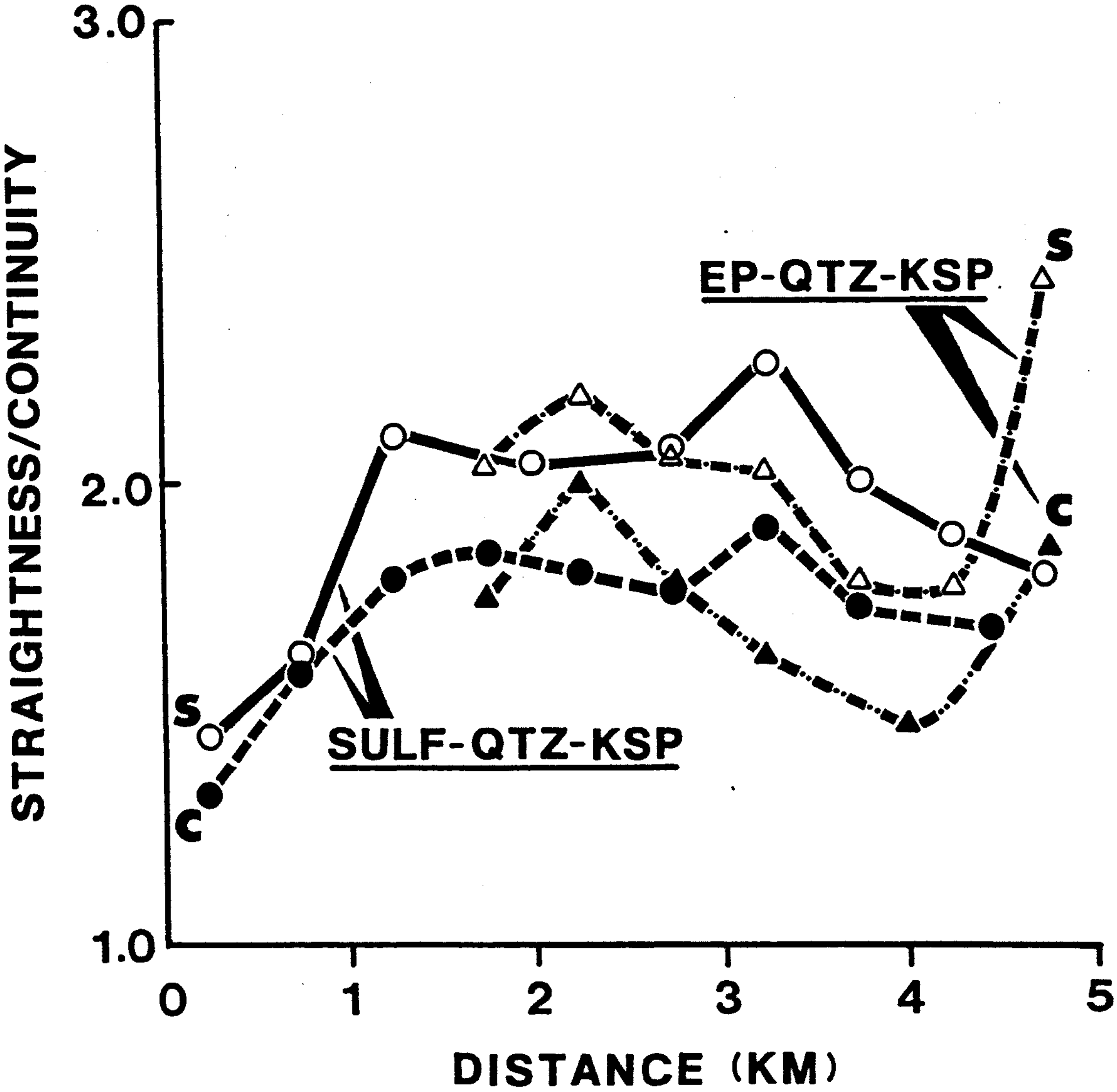

Figure 25. Straightness and Continuity versus Distance for the Early Alteration Assemblages. -- Origin corresponds to fracturing epicenter described in text. S=straightness, C=continuity.

coincident with the ENE and WNW regional trends are generally straighter and more continuous than those with other orientations (Figure 24). Fracture style plotted as a function of distance from the proposed center generates dissimilar curves for the two assemblages (Figure 25). These curves are apparently more irregular than the counterpart curves for the younger alteration assemblages plotted as a function of distance from the quartz monzonite porphyry stock at Sierrita.

Chapter 9

DISCUSSION OF FRACTURING RELATED TO AN EARLY HYDROTHERMAL EVENT

Fracture Densities Corrected for Topographic Elevation

Fracture densities of the two early alteration assemblages corrected for the 2000 feet of vertical relief present in the study area were plotted as a function of distance from a given 1.3 kilometer depth estimate below the chosen fracturing epicenter (Figure 26). The purely speculative basis of this depth figure is an attempt to match the slope and magnitude of the sulfide+quartz+K-feldspar curve with the curve of its Sierrita-related counterpart -- the quartz+sulfide assemblage. This counterpart curve is included on Figure 26 for comparison purposes.

Fracture Style Curves Corrected for Topographic Elevation

Fracture style corrected for topographic elevation generates relatively consistent curves for the nonsulfide and sulfide alteration assemblages (Figure 27). The general pattern displayed by the fracture style curves reveals the irregular, discontinuous fractures which dominate the most densely fractured region. With increasing distance from this suspected epicenter, fracture style remains relatively

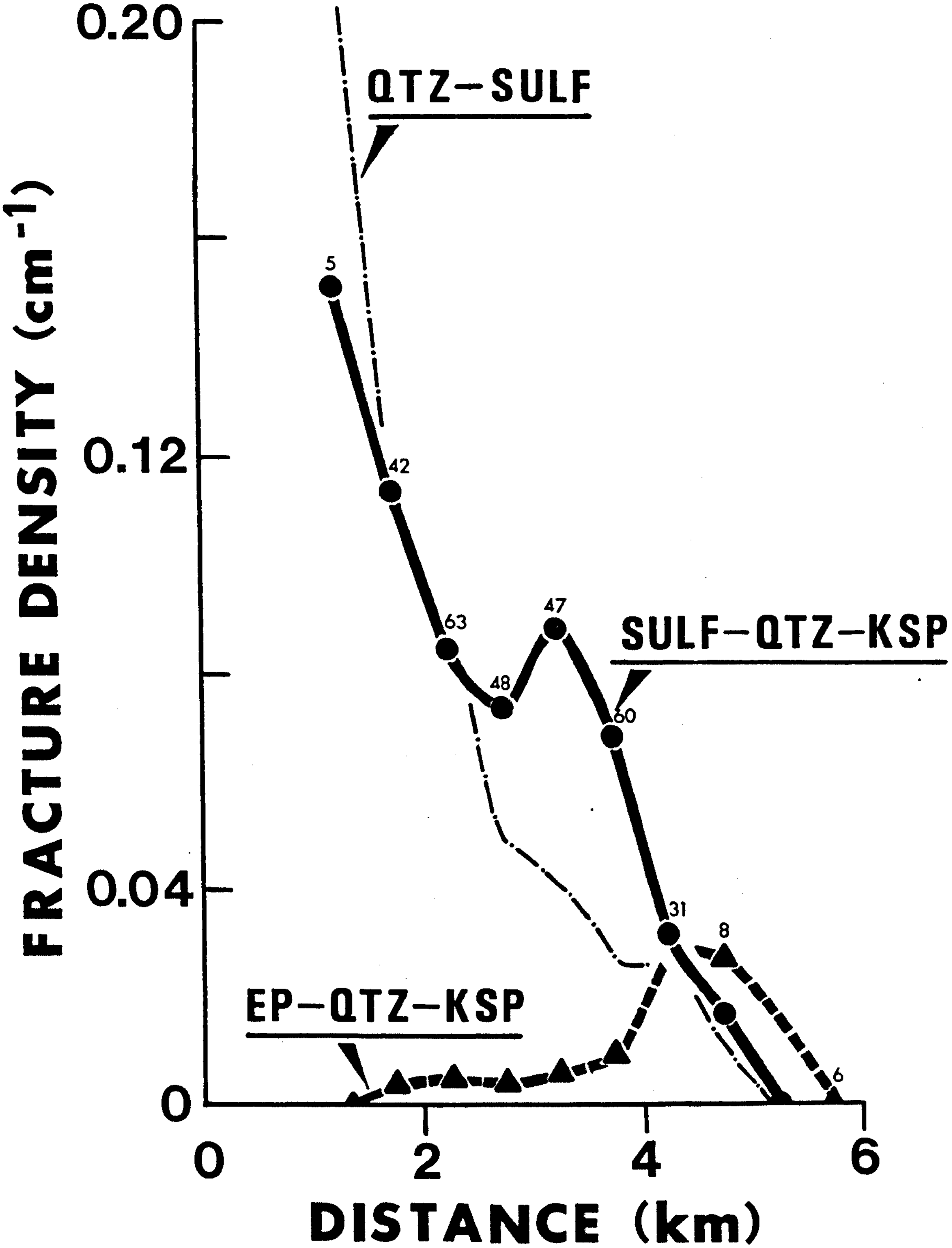

Figure 26. Fracture Density versus Distance Corrected for Elevation. -- The Quartz+Sulfide versus distance from the Sierrita center curve is included for comparison purposes.

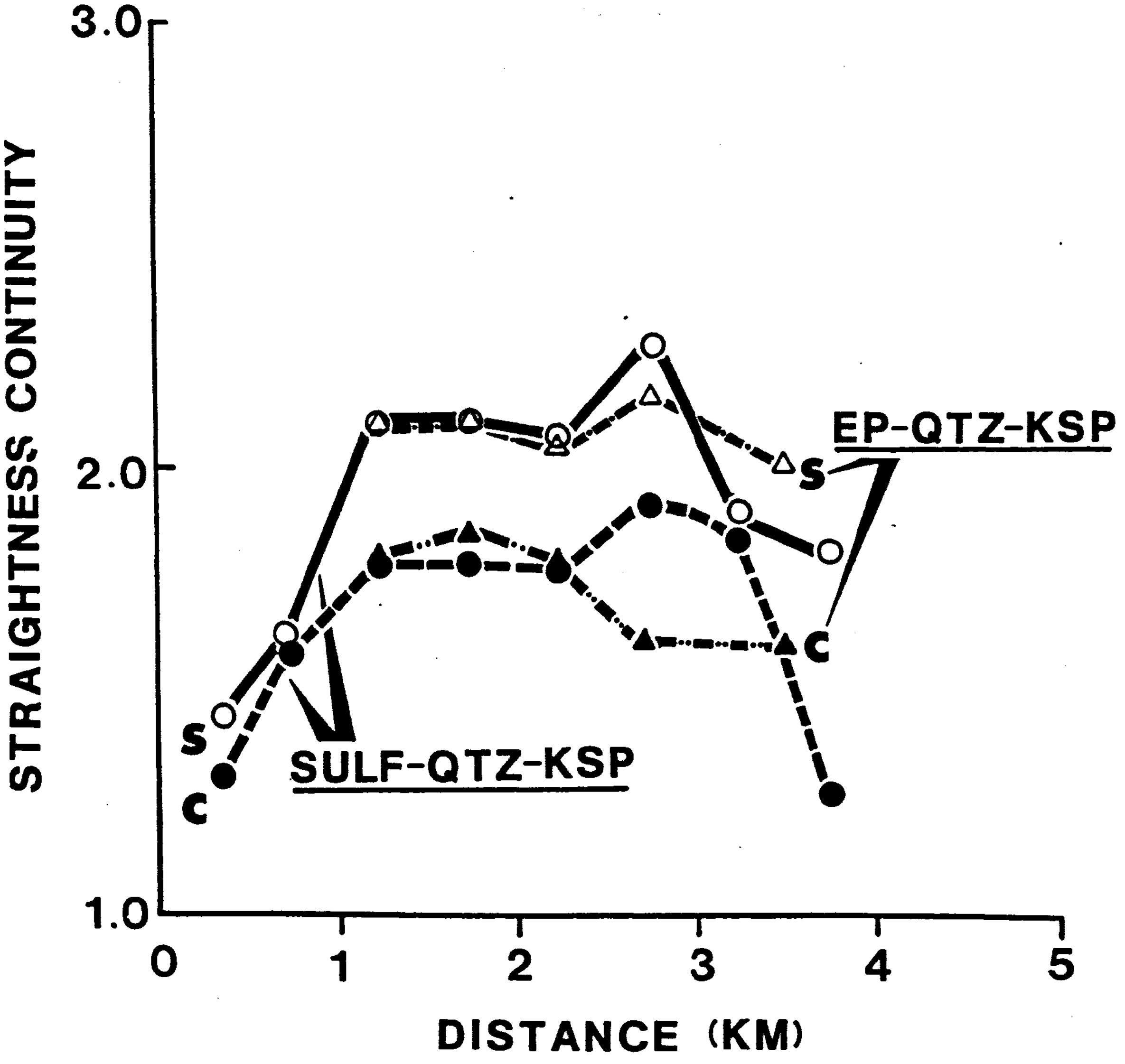

Figure 27. Straightness and Continuity versus Distance Corrected for Elevation. S=straightness; C=continuity.

consistent, peaking somewhat in the vicinity of the concentric arc of high density fracturing (Figure 22), and then decreasing abruptly, indicating an increase in the relative abundance of irregular, discontinuous fractures in the periphery of the system.

Fracture Strike Directions: Radial and Concentric Fracturing

The distribution of fracture orientations for the sulfide+quartz+K-feldspar assemblage in the Demetrie and Ox Frame Volcanics suggests the possibility of radial and concentric fracturing in these older volcanic rocks. Figure 28 is a graphic depiction of the spatial distribution of preferred orientations of the sulfide assemblage, excluding the Red Boy Rhyolite, and with the ENE regional trend removed. Each line represents an average preferred strike direction, as constituted by two or more subparallel fractures at a specific station site. The center of each line corresponds to the map location of that field station. Strike directions of N70E $\pm$ 5^{o} were not plotted in an attempt to eliminate this regional trend from consideration. Figure 29 presents a more quantitative examination of fracture patterns in the older volcanic units. Utilizing a coordinate system centered on the region of highest fracture densities of the sulfide assemblage (Figure 22), fracture strike direction is plotted as a function of the azimuth angle between field station sites and the origin. These two diagrams suggest that the preponderance of strike directions of the sulfide+quartz+K-feldspar assemblage in the Demetrie and Ox Frame Volcanics approximate crude radial and concentric fracture patterns.

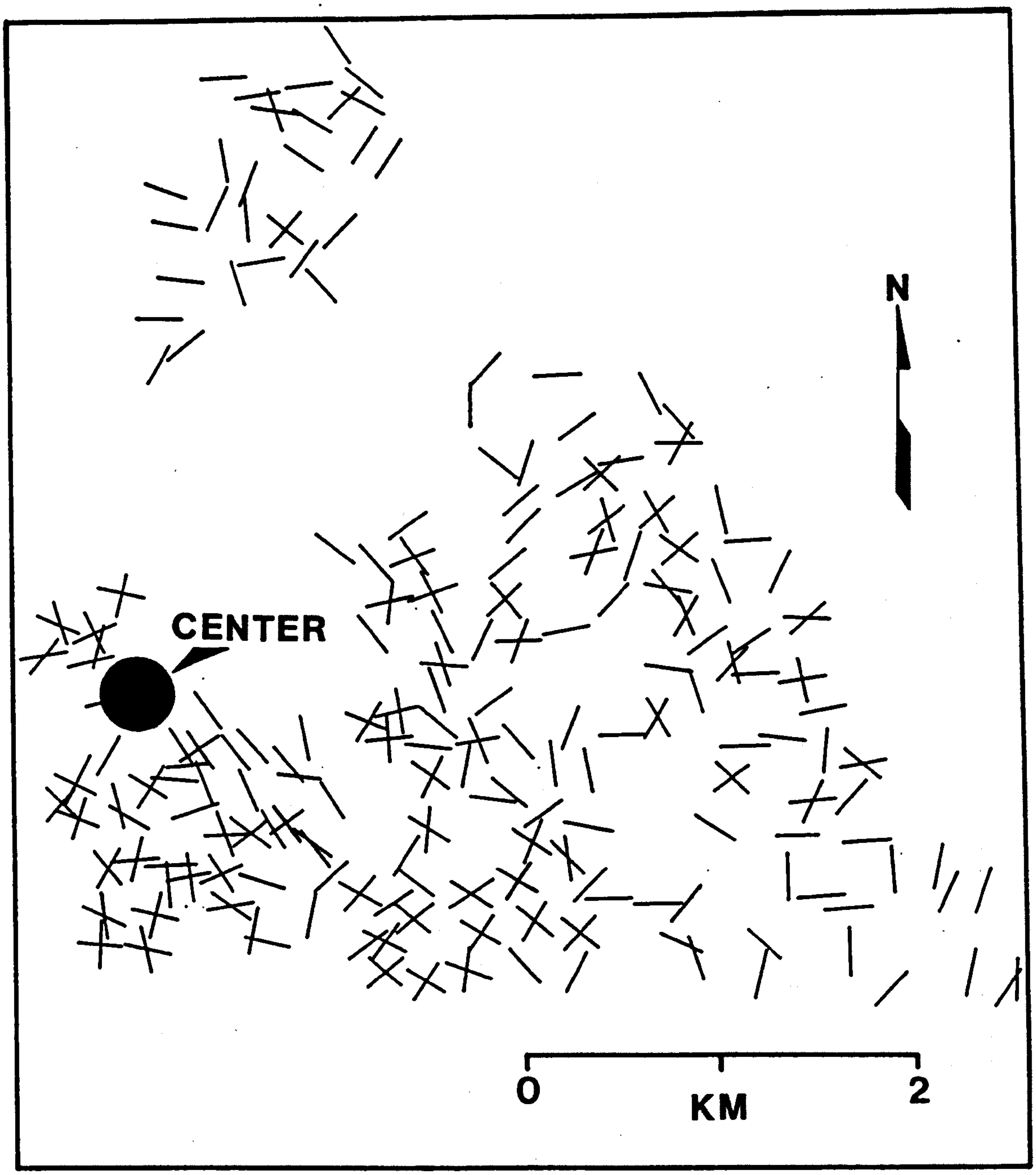

Figure 28. Plan Map of Dominant Strike Directions of the Sulfide+Quartz+K-feldspar Alteration Assemblage. -- The location of the center was based on the fracture density contour diagram for this same alteration assemblage (Figure 22). Fractures of N70E $\pm$ 5° and all fractures in the Red Boy Rhyolite are not included.

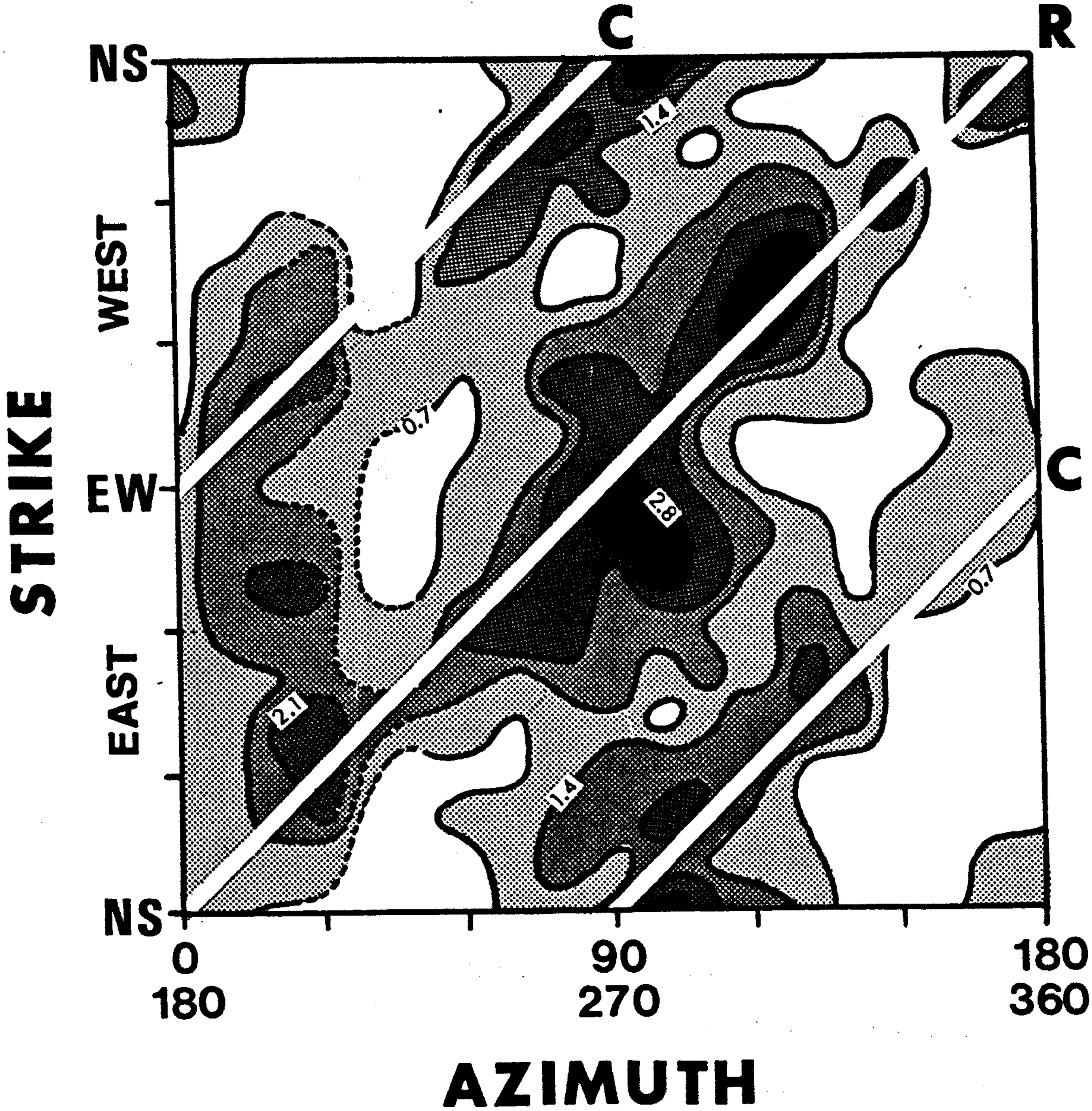

Figure 29. Azimuth Angle versus Strike Direction. -- The azimuth angle is the angle between the proposed center and the field station site. This angle is plotted against strike direction for fractures measured at that station. The white lines indicate the theoretical positions occupied by radial (R) and concentric (C) fracture orientations. Contours are per 1% of diagram area. Contour interval=0.7%. Intervals of 0.7%, 0.14%, 0.21%, and 0.28% are included on the diagram.

Lithologic Influence on Fracture Formation

The Red Boy Rhyolite, which caps the crest of the Sierrita Mountains, exhibits several geologic features that distinguish it from the older Mesozoic volcanic rocks (Figure 30). The first five observations have been documented previously by Cooper (1971, 1973).

1. The greatest observed thickness occurs at Red Boy Peak, the type section.
2. The Red Boy Rhyolite is metamorphosed north of Lobo Peak, in the core of the Sierrita Mountains.
3. Exposures in the high part of the range occur in a complex graben that narrows to the north-northeast, and may have formed, in part, during deposition of the rhyolite.
4. Lobo Peak, located about a mile south of Red Boy Peak, is a probable volcanic neck.
5. Zones of hydrothermal alteration present in the Demetrie Volcanics adjacent to Red Boy Peak apparently terminate at the contact with the Red Boy Rhyolite.
6. The two early fracture-controlled alteration assemblages are present in the Red Boy Rhyolite, although demonstrating relatively low fracture densities. The greatest fracture densities observed in the Red Boy Rhyolite occur at the southern flank of Red Boy Peak.

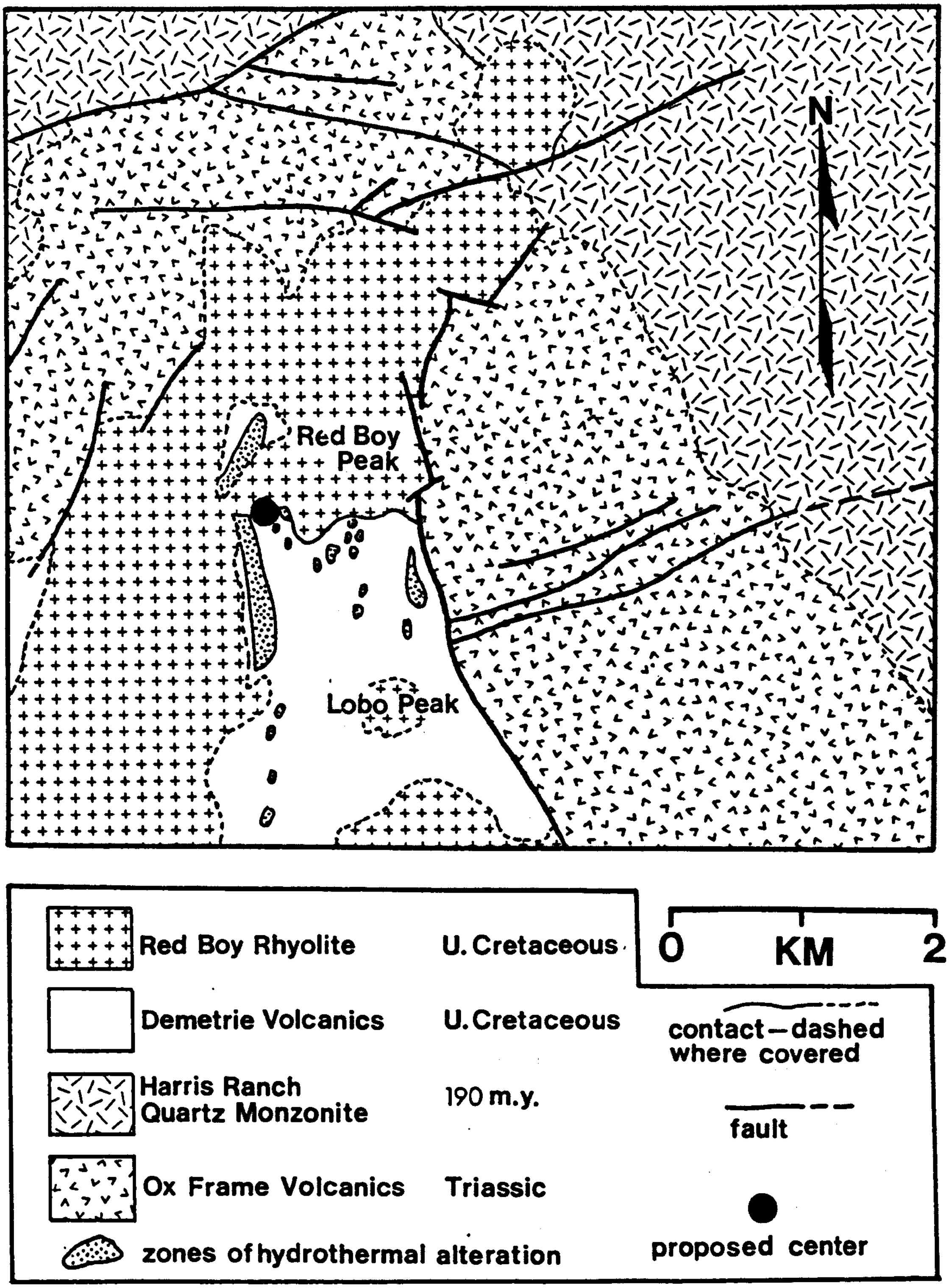

Figure 30. Generalized Geology in the Vicinity of the Fracturing Epicenter.

7. Fracture orientations of the sulfide assemblage are dominated by regional ENE double maxima, in contrast with the general lack of orientation maxima of this assemblage.

Evolution of Fractures

Two, relatively early fracture-controlled alteration assemblages are present in the Mesozoic volcanic rocks that are spatially distributed about a center eight kilometers west of the quartz monzonite porphyry stock at Sierrita. The first alteration assemblage, epidote+quartz+K-feldspar, is related to veins that attained moderate to low fracture densities, and a widespread, but irregular distribution. The second alteration assemblage, sulfide+quartz+K-feldspar, is controlled by fractures that exhibit high densities, is relatively restricted in areal extent, and displays an ordered distribution about a fracturing epicenter in the southwest corner of the study area. Irregular and discontinuous fractures dominate this densely fractured region and are also relatively abundant toward the periphery of the system.

On the basis of paragenetic relationships, fracture distribution patterns and orientations, and fluid inclusion temperatures (White, 1980) it has been proposed that the quartz+epidote+K-feldspar and sulfide+quartz+K-feldspar fracture-controlled alteration assemblages represent a distinct, early hydrothermal event. A comparison of the characteristics of these early assemblages with the relationship of the younger assemblages to the quartz monzonite porphyry stock implies a fundamentally different association of the early hydrothermal event to the Sierrita generator stock, or, perhaps more likely, that the early event represents a separate system altogether.

The spatial distribution of fracture densities and orientations of the two early assemblages suggest some speculations concerning phenomena responsible for fracture formation. Radial and concentric fracture patterns are predicted to form above a pluton during emplacement and cooling (Koide and Bhattacharji, 1975; Knapp and Norton, in press). The localization of high fracture densities at a center about which radial and concentric fracture patterns apparently exist implies a pluton at depth controlling fracture formation. Previously described geologic characteristics peculiar to the Red Boy Rhyolite and the vicinity of the proposed fracturing epicenter (Figure 30 and 31) prompts speculation that the upper Cretaceous rhyolitic unit may represent the volcanic equivalent of a plutonic body at depth that acted as an energy source producing hydrothermal alteration and fracture-controlled alteration assemblages centered near Red Boy Peak.

Figure 31. View of Red Boy Peak. -- Hill in foreground is Lobo Peak.

Chapter 10

OTHER FRACTURES

A fifth fracture-controlled alteration assemblage was observed in the Mesozoic volcanic rocks, consisting solely of calcite. Fractures of other alteration assemblages were often coated with calcite, which is probably forming even today. This calcite assemblage was measured in the western domain, as were barren fractures, and densities of both were plotted as a function of distance from the Sierrita generator stock (Figure 32). Fracture orientation data indicate a weak NNW maximum for both sets, with an additional WNW maximum for the calcite assemblage (Figure 33). The calcite assemblage was principally observed in a belt three to four kilometers from the Sierrita center, and in and near faults. Barren fractures display highly erratic densities on a local scale, but when averaged over one-half kilometer intervals exhibit very low but consistent fracture densities.

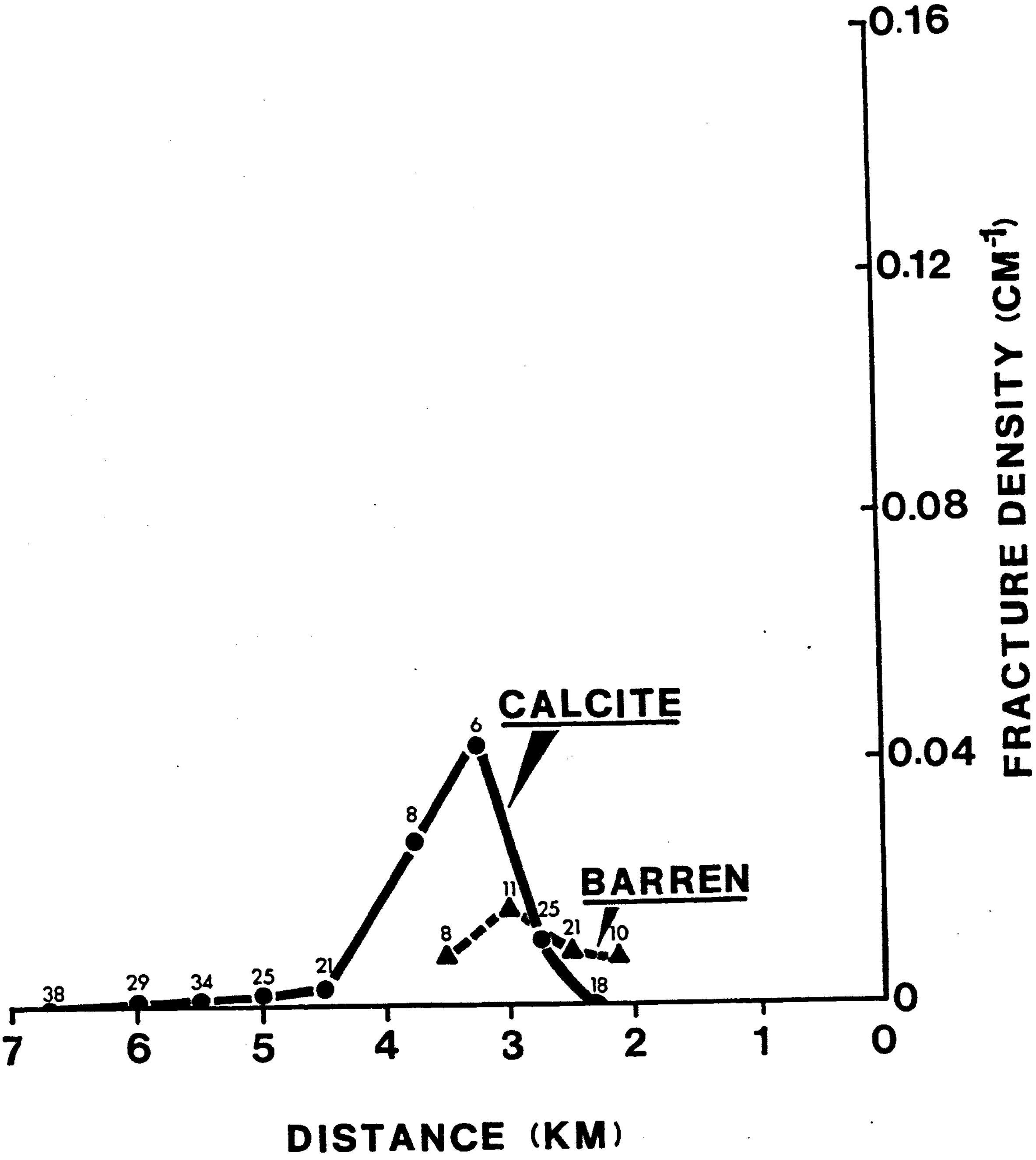

Figure 32. Fracture Density versus Distance for the Calcite Alteration Assemblage and Barren Fractures. -- Data on these assemblages was collected in the western domain only. Data on barren fractures was only collected for distances of about 3.5 kilometers from the Sierrita center. The number above each data point is the number of stations in that interval.

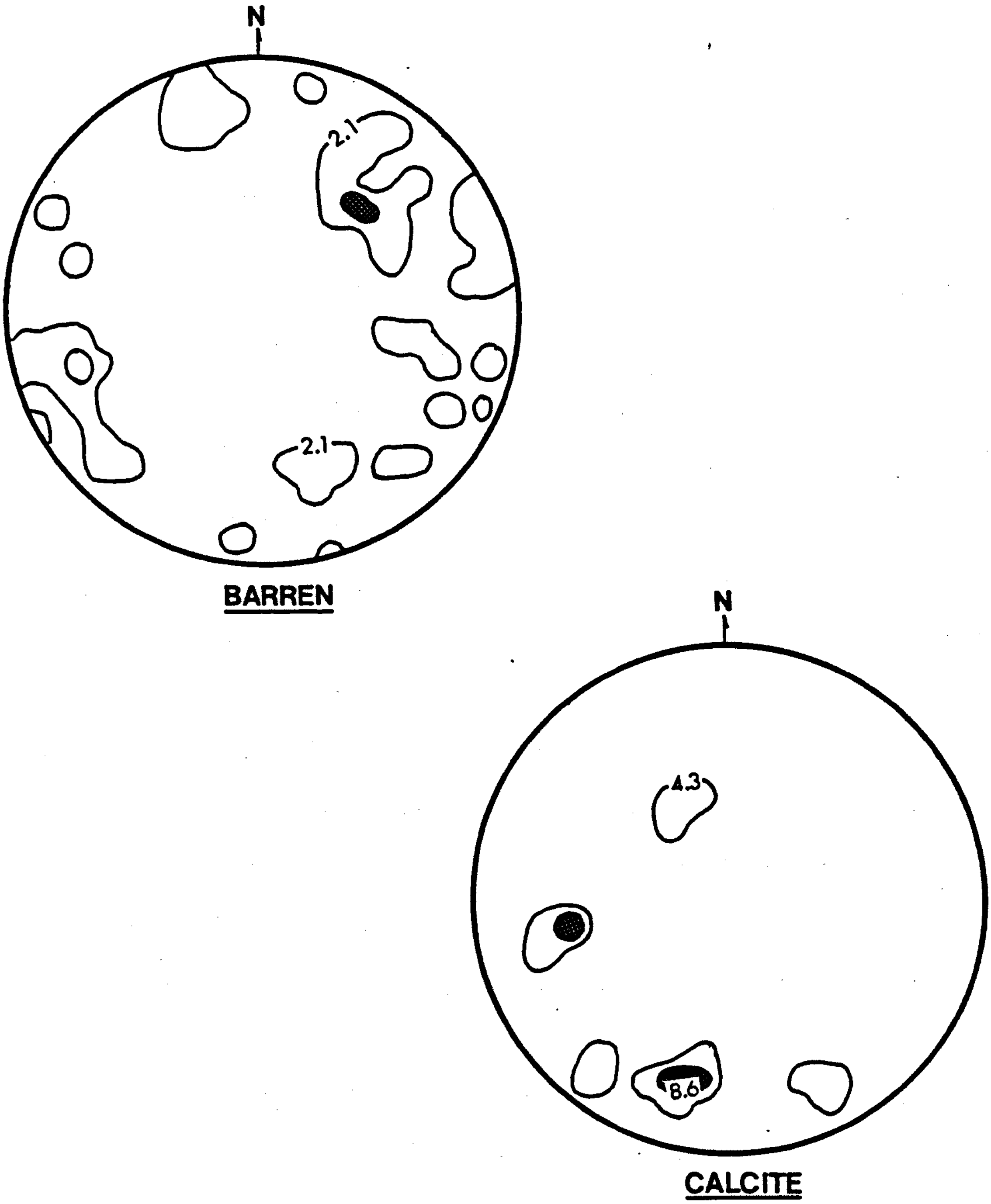

Figure 33. Fracture Orientations of the Calcite Alteration Assemblage and Barren Fractures. -- Contoured per 1% of area. Barren=191 points; Calcite=70 points.

Chapter 11

COMPARISONS WITH THE HARRIS RANCH QUARTZ MONZONITE AND RUBY STAR GRANODIORITE

The younger alteration assemblages in the Mesozoic volcanic rocks, quartz+epidote+K-feldspar and quartz+sulfide, have paragenetic equivalents in the Ruby Star Granodiorite (Table 1). The nonsulfide assemblage was not observed by White (1980) in the Harris Ranch Quartz Monzonite west of the Sierrita open pit, but was documented by Preece (1979) in the pit. Mineralogies, fracture densities, and fracture orientations of these two assemblages follow the same general patterns in all three rock types. The similarities are most striking with respect to the sulfide assemblage with almost identical fracture distributions generated in the intrusive and volcanic rocks. A late, K-feldspar±epidote alteration assemblage present in low fracture densities in the intrusive rocks is absent in the Mesozoic volcanic rocks, dying out north of the present study area (White, personal communication).

The principal differences in altered fractures between the various rock types is in the two early assemblages. The first set, epidote+quartz+K-feldspar, is present in the Harris Ranch Quartz Monzonite west of the Sierrita open pit, but absent in the Ruby Star

Granodiorite north of the open pits. The second assemblage, sulfide+quartz+K-feldspar, is present only in the Mesozoic volcanic rocks at distances over 3.5 kilometers west of the Sierrita center.

Chapter 12

APPLICATIONS TO THE EXPLORATION AND ORIGIN OF HYDROTHERMAL SYSTEMS

The "averaged" fracture density contour diagrams have exploration potential in locating a possible source of observed fracture-controlled alteration assemblages and evaluating the effects of faults and rock type on fracture formation. It is apparent from the present study that the contour diagrams of the sulfide-bearing assemblages are particularly effective in an exploration context. The strong fracture density gradients displayed by the quartz+sulfide assemblage about the quartz monzonite porphyry stock provide a definite focus on that Sierrita generator stock. The nonsulfide assemblage actually tends to obscure the location of a mineralizing center, both by its widespread areal extent and irregular distribution.

The localization of high fracture densities and hydrothermal alteration about the quartz monzonite porphyry stock implies that this intrusive body acted as an energy source for these phenomena. The distinctive fracture distributions and orientations characteristic of the various fracture-controlled alteration assemblages suggests that fractures are integrally linked to the hydrothermal event responsible for the alteration. The link between fracturing and the hydrothermal event producing observed alteration is strengthened by the continuation of these characteristic fracture patterns for correlative assemblages in the intrusive host rocks to the north (Haynes and Titley, 1980; Manske, 1980; White, 1980). This reasoning has potential for providing physical constraints on the evolution of a hydrothermal event through studies of fractures controlling alteration, just as the alteration mineralogy is determined by the chemical evolution of geothermal systems.

Chapter 13

SUMMARY AND CONCLUSIONS

Five fracture-controlled alteration assemblages are present in the Mesozoic volcanic rocks south and west of the Sierrita porphyry system. An early epidote+quartz+K-feldspar assemblage is followed by a sulfide+quartz+K-feldspar assemblage. This nonsulfide-sulfide sequence is repeated by two later alteration assemblages, quartz+ epidote+K-feldspar crosscut by a quartz+sulfide assemblage. These fracture-controlled alteration assemblages probably reflect two distinct hydrothermal systems. Fracture-controlled calcite postdates these four assemblages, and is often seen as a coating over them.

Fracture patterns developed in the two hydrothermal systems share many similarities, suggesting the following conclusions for the respective events.

1. A nonsulfide assemblage was produced early in the evolution of each system and is controlled by fractures attaining only moderate densities and relatively widespread, irregular distribution.
2. The early, nonsulfide assemblage is succeeded by an episode producing a sulfide alteration assemblage related to veins attaining higher fracture densities, but relatively restricted

areal extent. This assemblage displays strong fracture density gradients near the system center, with an increasingly irregular distribution toward the periphery of the system. The altered fractures are generally straighter and more continuous than altered fractures of the nonsulfide assemblage.

3. The importance of regional-tectonic stresses in controlling fracture geometry is reflected by ENE, WNW, NNW, and NE fracture orientation maxima. Radial and concentric fracturing is probably present for the early hydrothermal event, but if present about the Sierrita generator stock, it is masked by the regional trends.
4. Fractures throughout the system are generally traceable for 1.5 - 3.0 meters and display minor strike irregularities. Two areas, directly above the fracturing center west of Sierrita and toward the periphery of each system, are characterized by an abrupt increase in the relative abundance of irregular and discontinuous fractures. Fractures reflecting regional trends, especially those striking ENE, are generally straighter and more continuous than fractures of other orientations.
5. Rock type can have a pronounced effect on alteration mineralogy, fracture densities, and fracture style. Rock anisotropy generally appears not to have greatly influenced fracture orientation.

6. Faults can also influence fracture density distribution as is particularly evident in the sulfide assemblage in the more distal regions. The very high density fracture contours close to the center of the system, demonstrate little, if any deflection about faults.

From the spatial distribution and orientation of fractures it is possible to conclude that, at least for those fracture-controlled alteration assemblages associated with the Sierrita system, fracture formation has been controlled by the combined influences of regional tectonic stresses and the emplacement and cooling of a generator stock.

LIST OF REFERENCES

Aiken, M. A., and West, R. J., 1978, Some geologic aspects of the Sierrita-Esperanza copper-molybdenum deposit, Pima County, Arizona: Ariz. Geol. Soc. Dig., 11:117-128.

Anderson, C. A., 1948, Structural control of copper mineralization, Bagdad, Arizona: Trans. Am. Inst. Min. Met. Eng., 178: 170-180.

Batzle, M. L., and Simmons, G., 1976, Microfractures in rocks from two geothermal areas: Earth Planet Sci. Let., 30:71-93.

_______, 1977, Geothermal systems: rocks, fluid, fractures, in The Earths Crust, J. G. Heacock, ed., Am. Geophys. Union Mon. 20, pp. 233-242.

Cooper, J. R., 1960, Some geologic features of the Pima Mining District, Pima County, Arizona: U.S. Geol. Surv. Bull. 111-C.

_______, 1971, Mesozoic stratigraphy of the Sierrita Mountains, Pima County, Arizona: U.S. Geol. Surv. Prof. Paper 658-D, pp. D1-D40.

_______, 1973, Geological map of the Twin Buttes quadrangle, southwest of Tucson, Pima County, Arizona: U.S. Geol. Surv. Misc. Geol. Inv. Map I-745.

Damon, P. E., and Mauger, R. L., 1966, Epeirogeny-orogeny viewed from the Basin and Range Province: Soc. Min. Eng. Trans., 235:99-112.

Haynes, F. M., and Titley, S. R., 1980, The evolution of fracture-related permeability within the Ruby Star Granodiorite, Sierrita porphyry copper deposit, Pima County, Arizona: Econ. Geol., 75:673-683.

Heidrick, T. L., and Titley, S. R., in press, Fracture and dike patterns in Laramide plutons and their structural and tectonic implications, in Advances in Geology of the Porphyry Copper Deposits of Southwestern North America, Titley, S. R., ed., The University of Arizona Press.

Knapp, R. B., and Knight, J. E., 1977, Differential thermal expansion of pore fluids; fracture propagation and micro-earthquake production in hot pluton environments: Jour. Geophys. Res., 82:2515-2522.

Knapp, R. B., and Norton, D. L., in press, Preliminary numerical analysis of processes related to magma crystallization and stress evaluation in cooling pluton environments: Am. Jour. Sci.

Koide, H., and Bhattacharji, S., 1975, Formation of fractures around magmatic intrusions and their role in ore localization: Econ. Geol., 70:781-799.

Lacy, W. C., 1959, Structure and ore deposits of the east side of the Sierrita Mountains: Ariz. Geol. Soc. Dig., Vol. 2, p. 185.

Lynch, D. W., 1966, The economic geology of the Esperanza Mine and vicinity, in Geology of the Porphyry Copper Deposits -- Southwestern United States, S. R. Titley and C. L. Hicks, eds., Tucson: The University of Arizona Press, pp. 267-279.

_______, 1968, The Geology of the Esperanza Mine, Arizona: Ariz. Geol. Soc. Guidebook III, Tucson, p. 125-136.

Manske, Scott Lee, 1980, Fracturing events in the Ruby Star Granodiorite adjacent to the Esperanza prophyry copper deposit, Pima County, Arizona, The University of Arizona, M. S. Thesis, 102 p.

Norton, D., and Knight, J. E., 1977, Transport phenomena in hydrothermal systems: cooling plutons: Am. Jour. Sci., 277: 937-981.

Preece, R. K., 1979, Contrasting evolutions of hydrothermal alteration in quartz monzonite and quartz diorite at the Sierrita porphyry copper deposit, Arizona: The University of Arizona, M.S. Thesis, 106 p.

Rehrig, W. A., and Heidrick, T. L., 1972, Regional fracturing in Laramide stocks of Arizona and its relationship to porphyry copper mineralization: Econ. Geol., 67:198-213.

_______, 1976, Regional tectonic stress during the Laramide and late Tertiary intrusive periods, Basin and Range province, Arizona: Ariz. Geol. Soc. Digest 10, p. 205-228.

Smith, V. L., 1975, Hypogene alteration at the Esperanza Mine, Pima County, Arizona: M. S. Thesis, The University of Arizona.

Snow, D. T., 1970, The frequency and apertures of fractures in rock: Intnl. Jour. Rock Mech. Min. Sci., 7:23-40.

Titley, S. R., 1978, Geologic history, hypogene features, and processes of secondary sulfide enrichment at the Plesyumi copper prospect, New Britain, Papua New Guinea: Econ. Geol., 73:768-784.

Titley, S. R., Fleming, A. W., and Neale, T. I., 1978, Tectonic evolution of the porphyry copper system at Yandera, Papua New Guinea: Econ. Geol. , 73:810-828.

Weaver, R. R., 1971, Uplift and gravitational adjustment in the Ruby Star Ranch area, Pima mining district, Arizona: Ariz. Geol. Soc. Digest, Vol. 9, pp. 197-211.

White, J. L., Research Assitant, University of Arizona, Tucson, Arizona, Personal Communication.

_______, 1980, The development of fractures in the Harris Ranch Quartz Monzonite related to the Sierrita porphyry copper system, Pima County, Arizona, M.S. Thesis, The University of Arizona.

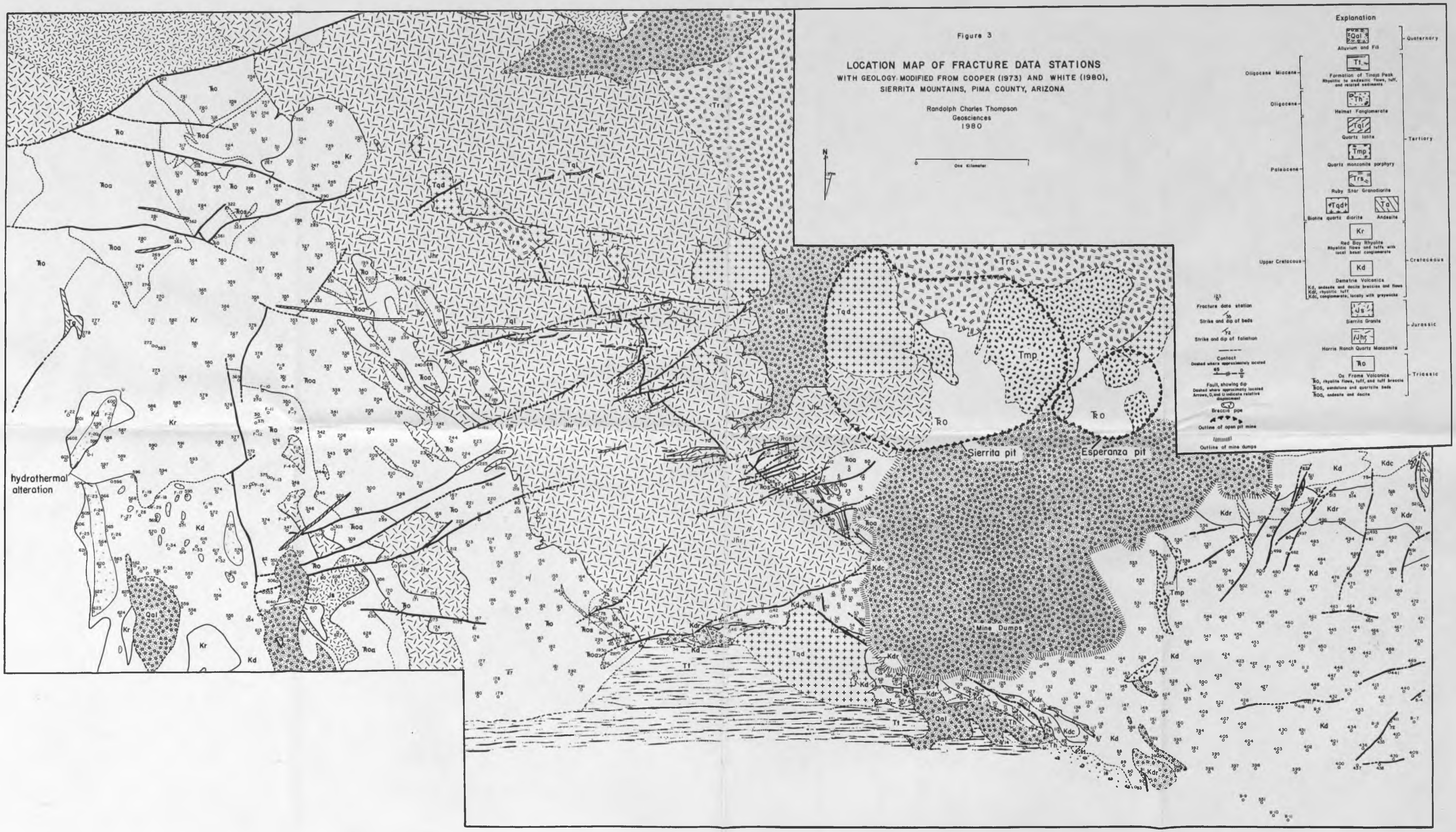
Figure 3
LOCATION MAP OF FRACTURE DATA STATIONS
WITH GEOLOGY MODIFIED FROM COOPER (1973) AND WHITE (1980),
SIERRITA MOUNTAINS, PIMA COUNTY, ARIZONA
Randolph Charles Thompson
Geosciences
1980
N
0
One Kilometer
Explanation
Qal
Alluvium and Fill
Quaternary
Oligocene Miocene
Tt
Formation of Tinaja Peak
Rhyolitic to andesitic flows, tuff, and related sediments
Oligocene
Th
Helmet Fanglomerate
Tql
Quartz latite
Tertiary
Tmp
Quartz monzonite porphyry
Paleocene
Trs
Ruby Star Granodiorite
Tqd
Biotite quartz diorite
Ta
Andesite
Kr
Red Boy Rhyolite
Rhyolitic flows and tuffs with local basal conglomerate
Upper Cretaceous
Cretaceous
Kd
Demetrie Volcanics
Kd, andesite and dacite breccias and flows
Kdr, rhyolitic tuff
Kdc, conglomerate, locally with greywacke
Js
Sierrita Granite
Jurassic
Jhr
Harris Ranch Quartz Monzonite
Ro
Ox Frame Volcanics
Triassic
Ro, rhyolite flows, tuff, and tuff breccia
Ros, sandstone and quartzite beds
Roa, andesite and dacite
Fracture data station
Strike and dip of beds
Strike and dip of foliation
Contact
Dashed where approximately located
Fault, showing dip
Dashed where approximately located
Arrows, D, and U indicate relative displacement
Breccia pipe
Outline of open pit mine
Outline of mine dumps
Sierrita pit
Esperanza pit
Mine Dumps
hydrothermal alteration